MOLECULAR AND CELLULAR BIOLOGY, May 1998, p. 3044–3058 Vol. 18, No. 5
0270-7306/98/$04.00+0

Activation of Rho-Dependent Cell Spreading and Focal Adhesion Biogenesis by the v-Crk Adaptor Protein

ZEYNEP F. ALTUN-GULTEKIN,[1]† SANJAY CHANDRIANI,[2] CECILE BOUGERET,[2] TOSHIMASA ISHIZAKI,[3] SHUH NARUMIYA,[3] PETRA DE GRAAF,[4] PAUL VAN BERGEN EN HENEGOUWEN,[4] HIDESABURO HANAFUSA,[2] JOHN A. WAGNER,[1] AND RAYMOND B. BIRGE[2]*

Department of Neurology and Neuroscience, Cornell University Medical College,[1] and Laboratory of Molecular Oncology, The Rockefeller University,[2] New York, New York; Second Department of Pharmacology, Faculty of Medicine, Kyoto University, Kyoto, Japan[3]; and Department of Molecular Cell Biology, Utrecht University, Utrecht, The Netherlands[4]

Received 1 October 1997/Returned for modification 12 November 1997/Accepted 2 February 1998

The small GTPase RhoA plays a critical role in signaling pathways activated by serum-derived factors, such as lysophosphatidic acid (LPA), including the formation of stress fibers in fibroblasts and neurite retraction and rounding of soma in neuronal cells. Previously, we have shown that ectopic expression of v-Crk, an SH2/SH3 domain-containing adapter proteins, in PC12 cells potentiates nerve growth factor (NGF)-induced neurite outgrowth and promotes the survival of cells when NGF is withdrawn. In the present study we show that, when cultured in 15% serum or lysophosphatidic acid-containing medium, the majority of v-Crk-expressing PC12 cells (v-CrkPC12 cells) display a flattened phenotype with broad lamellipodia and are refractory to NGF-induced neurite outgrowth unless serum is withdrawn. v-Crk-mediated cell flattening is inhibited by treatment of cells with C3 toxin or by mutation in the Crk SH2 or SH3 domain. Transient cotransfection of 293T cells with expression plasmids for $p160^{ROCK}$ (Rho-associated coiled-coil-containing kinase) and v-Crk, but not SH2 or SH3 mutants of v-Crk, results in hyperactivation of $p160^{ROCK}$. Moreover, the level of phosphatidylinositol-4,5-bisphosphate is increased in v-CrkPC12 cells compared to the levels in mutant v-Crk-expressing cells or wild-type cells, consistent with PI(4)P5 kinase being a downstream target for Rho. Expression of v-Crk in PC12 cells does not result in activation of Rac- or Cdc42-dependent kinases PAK and S6 kinase, demonstrating specificity for Rho. In contrast to native PC12 cells, in which focal adhesions and actin stress fibers are not observed, immunohistochemical analysis of v-CrkPC12 cells reveals focal adhesion complexes which are formed at the periphery of the cell and are connected to actin cables. The formation of focal adhesions correlates with a concomitant upregulation in the expression of focal adhesion proteins FAK, paxillin, α_3-integrin, and a higher-molecular-weight form of β_1-integrin. Our results indicate that v-Crk activates the Rho-signaling pathway and serves as a scaffolding protein during the assembly of focal adhesions in PC12 cells.

Various cellular functions such as cell motility, cell survival, cytokinesis, and neurite outgrowth are dependent on temporal and spatial reorganization of the actin cytoskeleton. Rearrangement of the actin cytoskeleton results from signals activated by soluble factors (inside-out signals) and cell-substratum and cell-cell adhesion molecules (outside-in signals). In cultured cells, integration of these signals takes place in the focal adhesions (58) which are associated with well-defined actin stress fibers and provide tight binding to the underlying extracellular matrix. These contractile stress fibers are postulated to exert tension on the substratum and to play a role in morphogenesis and regulate cell motility.

Actin stress fibers and focal adhesions form in quiescent fibroblasts in response to microinjection of constitutively active Rho GTPase or by extracellular signals such as lysophosphatidic acid (LPA) and bombesin (62) which lead to the activation of Rho. ADP-ribosylation and inhibition of Rho by *Clostridium botulinum* C3 toxin prevent this process. During focal adhesion assembly, several adhesion-associated proteins, including focal adhesion kinase (FAK), paxillin, and $p130^{cas}$, become tyrosine phosphorylated, suggesting the involvement of a tyrosine phosphorylation cascade in this event (9, 65, 77). LPA-induced activation of Rho can be blocked by an inhibitor of tyrosine kinase signaling, tryphostin, suggesting that tyrosine kinases act upstream of Rho activation (57). However, it has also been demonstrated that introduction of activated Rho into cells induces tyrosine phosphorylation of FAK, paxillin, and $p130^{cas}$, placing tyrosine kinases downstream of Rho (18). To further support this concept, another tyrosine kinase inhibitor, genistein, prevents the formation of stress fibers after microinjection of constitutively active Rho (61). Besides serum-derived factors, binding of integrins to extracellular matrix proteins also activates Rho and induces stress fiber formation in the absence of serum (4). It is currently not well understood how integrin engagement, tyrosine kinase signaling, Rho activation, and formation of focal adhesions are integrated and coordinated at the cell membrane.

According to a recent model, intracellular components of the focal adhesion complex and actin filaments associate with integrins upon integrin engagement with the extracellular matrix. In the presence of active Rho, these complexes and actin cluster by acto-myosin contraction, which leads to focal adhe-

* Corresponding author. Mailing address: The Rockefeller University, 1230 York Ave., New York, NY 10021. Phone: (212) 327-7412. Fax: (212) 327-7943. E-mail: birger@rockvax.rockefeller.edu.

† Present address: Department of Pathology, Robert Wood Johnson Medical School, Piscataway, NJ 08854-5635.

sion and stress fiber formation (13). Furthermore, this is thought to stimulate FAK activation within the complexes in a manner similar to receptor tyrosine kinase autophosphorylation and activation (8). Supporting this model, among various Rho effector proteins such as Rhotekin, Rhofilin, protein kinase N, Citron, p140mDia, PRK2, phosphatidylinositol-4-phosphate 5-kinase [PI(4)P5-kinase], and Rho-kinases (ROKα/Rho-kinase, ROKβ/p160^{ROCK}) (31, 43, 48, 59, 60, 74–76), activation of Rho-kinase causes myosin light-chain phosphorylation, which may stimulate acto-myosin contraction (36). In addition, activation of another Rho effector, PI(4)P5-kinase, leads to increased phosphatidylinositol-4,5-bisphosphate [PI(4,5)P_2] levels, which facilitates the dissociation of profilin and gelsolin from actin and allows net actin polymerization (35).

Nerve growth factor (NGF)-induced neurite outgrowth is controlled by the Rho family of GTPases at the structural level. Previously, we have shown that Rac activity is required for neurite elongation and tension formation in the axon (2, 40). In contrast, Rho activity was found to be inhibitory for neurite outgrowth since it caused growth cone collapse as well as cell rounding in native PC12 cells (34, 71). Thus, it has been recently suggested that in contrast to fibroblasts, where Cdc42, Rac, and Rho work in a linear fashion (56), Rac and Rho have opposite actions on the cytoskeleton in neuronal cells (38). In the present study, we present evidence that the SH2/SH3 domain containing adapter protein v-Crk can participate in LPA signaling to RhoA, leading to biogenesis of focal adhesions and actin stress fibers in PC12 cells. These cytoskeletal effects appear to be concomitant with the ability of v-Crk to bind stably to focal adhesions and elevate the expression of specific focal adhesion proteins. Hence, our results raise the possibility that adapter proteins can act as scaffolds during the synthesis of focal adhesions and shape changes in neuronal cells.

MATERIALS AND METHODS

Construction of expression vectors, transfection, and cell lines. PC12 cells expressing v-Crk (clones V15 and V1) and R273N–v-Crk (an SH2 mutant of v-Crk) have been previously described (28, 70). To generate stable PC12 cell lines expressing SH3 mutants of v-Crk, we subcloned BSP–v-Crk cDNA (pCT10) carrying the D386DRHAD insertional mutation (51) into the pMEXneo mammalian expression vector. Briefly, an *Alw*NI fragment containing the entire coding region of mutant v-Crk was cloned into *Eco*RI-*Bam*HI-digested pMEXneo with *Bam*HI-*Eco*RI linkers, after which 20 μg of plasmid DNA was purified and transfected into PC12 cells by the Lipofectamine method. Stable cell lines of clonal origin were obtained and expanded as described previously (28). All constructs were sequenced prior to transfection to verify sequence integrity. To verify that D386DHRAD–v-Crk behaved as a loss-of-SH3-function mutant, wild-type v-Crk SH3 or D386DHRAD mutant SH3 domains were PCR amplified from the purified pMEXneo plasmid DNA with the forward primer 5′CCGTG CGGATCCGTGCGAGCTCTCTTTGACTTT3′ and the reverse primer 5′CTA ATTGAATTCTCTCGACGTAAGGAACAGGTA3′ engineered with 5′ *Bam*HI and 3′ *Eco*RI restriction sites, respectively. Following PCR amplification, clones were sequenced to verify sequence integrity and ligated into *Bam*HI-*Eco*RI-linearized pGEX-2TK plasmid DNA (Pharmacia). The glutathione *S*-transferase (GST), GST-CrkSH3, or GST-D386DHRAD-Crk SH3 fusion proteins were expressed in *Escherichia coli* DH5α cells after induction with 1 mM isopropyl-β-D-thiogalactopyranoside (IPTG) for 3 h at 37°C. The bacteria were lysed by sonication in bacterial lysis buffer (1% Triton X-100, 20 mM Tris-Cl [pH 7.5], 150 mM NaCl, 1 mM phenylmethylsulfonyl fluoride) and clarified by centrifugation at 8,500 × *g* for 20 min. GST fusion proteins were purified from the lysate over GSH-Sepharose resin (Pharmacia), eluted with 20 mM glutathione (GSH), dialyzed against phosphate-buffered saline (PBS), and stored at −70°C (17). pGEX-2TK contains the recognition sequence for the catalytic subunit of cyclic AMP-dependent protein kinase located between the GST domain and the multiple-cloning site. GST fusion proteins were labeled with purified bovine heart kinase (Sigma; P2645) and [γ-^{32}P]ATP (3,000 mCi/mmol) as specified by the manufacturer of pGEX-2TK (Pharmacia; 27-4587-01), and all fusion proteins were labeled to similar specific activities.

SH3 domain overlay assay. To quantify binding of v-Crk or D386DHRAD–v-Crk SH3 domains to proline-rich sequences, the high affinity Crk-binding sequence (CB1) derived from amino acids 282 through 294 in C3G (SPPPALPPKKRQ) was cloned into pGEX-2T and expressed as a GST fusion protein (37). As a control for binding specificity, a mutated sequence containing K10L (SPPPALPPKLRQ) was used in place of the wild-type sequence since it has been shown that lysine is absolutely required for Crk binding to CB1 (37). GST or GST fusion proteins (3.5 μg) containing CB1 or K10L-CB1 were separated by sodium dodecyl sulfate-polyacrylamide gel electrophoresis (SDS-PAGE) (12% polyacrylamide) and transferred to Immobilon P membranes. The membranes were incubated for 1 h at room temperature in blocking buffer (150 mM NaCl, 20 mM Tris-Cl [pH 7.5], 1% [wt/vol] bovine serum albumin [BSA]), rinsed with Tris-buffered saline, and incubated, with gentle shaking, at 4°C overnight with 5 μg of [^{32}P]GST or [^{32}P]GST-SH3 domains per ml in SH3 overlay solution containing 1% BSA, 20 mM Tris-Cl (pH 7.4), 1 mM dithiothreitol, and 0.1% Tween 20. The filters were washed three times, and bound radioactivity was detected by autoradiography.

Tissue culture and stimulation of cells. PC12 cells and all v-Crk subclones were maintained in Dulbecco's modified Eagle's medium (DMEM; Gibco BRL) containing 10% horse serum and 5% calf serum (Gemini Bioproducts, Inc.) and incubated in a humidified atmosphere at 37°C under 5% CO_2. To isolate v-Crk-expressing flat cells (V15F and V1F) from round (V15R and V1R) cells, the cells were plated in 75-cm^2 flasks with screw caps, and after 12 h round cells were lifted off the substratum by slight manual trituration of the cells. Medium containing the floating round cells was then transferred to another flask, and the flask containing the flat cells was washed twice with medium to remove any remaining round cells. To ADP-ribosylate and inhibit Rho, 100 μg of C3 toxin per ml was added directly to the culture medium and the cells were treated for 12 h (34, 39) before any further treatment. For serum starvation assays, the cells were plated in serum-containing medium and 24 h later were switched to defined DMEM which contained 5 μg of insulin per ml, 5 μg of transferrin per ml, 10^{-4} M putrescine, 20 nM progesterone, 30 nM sodium selenite, and 1 U of thrombin per ml (all chemicals from Sigma). The cells were kept in defined DMEM overnight before any treatment. For morphological assays, 1 μM LPA (Sigma), 15% serum (Gibco BRL), or 100 ng of NGF (Collaborative Biomedicals) per ml was added to the culture medium for the indicated times. Since insulin can activate tyrosine kinase receptors which may activate Rho family GTPases, we also tested DMEM without insulin and obtained similar results. Phase-contrast photographs of cells were taken through a Zeiss Axiovert 100 microscope equipped with an Achrostigmat Ph1 objective (32×, 0.4 numerical aperture) and a camera with Kodak T-max 100 film. To measure the changes in cell surface areas, we photographed random areas of cells under each treatment protocol. These photographs were then scanned with a Nikon Scantouch and Adobe Photoshop software. The contours of individual cells on each photograph were then marked, and their surface area was measured with NIH image software. The raw data obtained by this procedure was then processed for statistical analysis.

TLC and HPLC analysis of PIP2 levels. Phospholipid labeling and extractions were based on the thin-layer chromatography (TLC) method (11). Briefly, equivalent numbers of cells were maintained in 15% serum in phosphate-free DMEM and labeled for 16 h with 20 μCi of [^{32}P]orthophosphate. The cells were washed with PBS and lysed in acidic chloroform-methanol. The organic phase was reextracted with 100 mM EDTA in acidic chloroform-methanol and dried under N_2. Lipids were separated by TLC with commercial, nonradioactive PI(4)P and PI(4,5)P_2 as markers in a chloroform–methanol–4.3 M ammonium hydroxide (9:7:2) solvent system. The TLC plates were analyzed with a phosphorimager (PhosphoroImager SI; Molecular Dynamics Inc., B&L Systems, Zoetermeer, The Netherlands). Spots were quantified with ImageQuaNT software, version 4.2, Microsoft for Windows. For high-pressure liquid chromatography (HPLC) analysis, extracted lipids were deacetylated with methylamine and compared with [^{3}H]PI(4)P, [^{3}H]PI(3,4)P_2, and [^{3}H]PI(4,5)P_2 standards.

Transient DNA transfections and kinase assays. 293T cells were transfected with the Stratagene MBS mammalian transfection kit (no. 200388), with minor modifications. Briefly, in 60-mm tissue culture plates, cells were plated at approximately 50% confluency in DMEM containing 10% fetal calf serum. After being washed in PBS, the cells were transfected with up to 6 μg of plasmid DNA containing either pMEX (control), pCMX-mycROCK, pMEX-*v-crk*, pJ3H-*PAK1*, pEXV-*V12rac1*, pEXV-*N19rhoA*, or pcEXV-*rhoA* in DMEM containing 6% modified bovine solution. In some experiments, cells were transfected with 0.3 μg of pEGFP (Clontech), a plasmid encoding the green fluorescent protein, so that transfection efficiency could be monitored at 485 nM with a fluorescein isothiocyanate emission filter. After 3 h in 6% modified bovine solution, the medium was changed to DMEM–10% fetal calf serum for an additional 30 h, after which the cells were lysed in 500 μl of nonionic lysis buffer containing 1% HNTG (20 mM HEPES, 150 mM NaCl, 1% Triton X-100, 10% glycerol). Samples were normalized for protein and clarified by centrifugation at 13,000 × *g* for 5 min, and 1 μg of anti-Myc antibody (monoclonal antibody [MAb] 9E10; Calbiochem no. OP10-Q) was added to lysates for 3 h, after which immune complexes were collected with rabbit anti-mouse antibody–Sepharose (Jackson Laboratories) beads for 1 h. After being washed three times with 0.1% HNTG, the beads were resuspended for 30 min with gentle agitation in 50 μl of kinase buffer containing 5 μCi of [γ-^{32}P]ATP, 2 μM cold ATP, 10 mM $MnCl_2$, and 5 μg of histone H1 as the substrate. To stop the reaction, 4× electrophoresis sample buffer was added and the mixture was boiled for 5 min. Samples were resolved by SDS-PAGE (8.5% polyacrylamide) and transferred to Immobilon P membranes (Millipore), and radioactivity was detected by autoradiography of the membranes. The membranes were subsequently immunoblotted with anti-Myc MAb to determine expression levels of myc-p160^{ROCK} fusion protein. To assay

the activation status of PAK65, JNK, and S6 kinase, native PC12 cells, v-Crk, R273N-v-Crk, or D386DRHAD–v-Crk cells were lysed as above and immunoprecipitated with either anti-PAK65 (provided by Gary Bokoch, Scripps Clinic, La Jolla, Calif.), anti-S6 kinase (provided by M. Chou and J. Blenis, Harvard University, Boston, Mass.), or commercial anti-JNK antibody (Santa Cruz no. 15701A). In vitro kinase assays were performed as above with 5 μg of myelin basic protein (MBP) for PAK65, S6 for S6 kinase, or GST containing the first 79 amino acids of c-Jun (22) for JNK.

Preparation of lysates and immunoblotting. To examine the expression levels of cytoskeletal proteins, detergent lysates of cells were prepared in RIPA buffer containing 50 mM NaCl, 10 mM Tris (pH 7.4), 1 mM EDTA, 1% Triton X-100, 1% sodium deoxycholate, and a cocktail of protease inhibitors (Complete; Boehringer Mannheim) or modified RIPA buffer containing 150 mM NaCl, 50 mM Tris (pH 7.4), 1% Nonidet P-40, 0.5% sodium deoxycholate, and protease inhibitors. Modified RIPA buffer was used for immunoblotting of integrins. After 15 min on ice, lysates were clarified by centrifugation in a microcentrifuge, and protein concentrations were quantified by the Bio-Rad protein assay. Equivalent amounts of protein-containing lysates were boiled in sample buffer under reducing or nonreducing (for α_5- and α_v-integrins) conditions and resolved by SDS-PAGE (6% polyacrylamide for FAK, vinculin, talin, and paxillin and 7.5% polyacrylamide for β_1-integrin, α-actinin, v-Crk, actin, α_5-integrin, $p130^{cas}$, α_3-integrin, and α_v-integrin), and immunoblotting was carried out as described previously (2). Briefly, the membranes were incubated for 4 h in 10 mM Tris (pH 7.4)–150 mM NaCl–10% Triton X-100 (wash solution) with 10% fetal calf serum to block nonspecific binding. They were then incubated in primary antibodies for 2 h at the following dilutions; talin, α-actinin, and vinculin (MAbs from Sigma) at 1:500; paxillin and FAK (MAbs from Transduction Labs) at 1:1,000; actin (MAb from Boehringer Mannheim) at 1:500; $p130^{cas}$ (MAb from Santa Cruz) at 1:1,000; α_3-integrin (polyclonal Ab provided by L. Reichardt, University of California, San Francisco) at 1:1,000; α_5-integrin (polyclonal Ab provided by F. Giancotti, Memorial Sloan-Kettering Cancer Center) at 1:500; α_v-integrin (polyclonal Ab from Chemicon International Inc.) at 1:1,000; and β_{1cyto}-integrin (polyclonal Ab provided by L. Reichardt) at 1:1,000. MAbs (anti-3C2) to the Gag region of v-Crk have been described previously (70). Following incubation with primary antisera, immunoblots were reblocked for 30 min and incubated in polyclonal horseradish peroxidase-conjugated anti-mouse or anti-rabbit (Amersham) antibodies for 90 min. The blots were processed and exposed to films by the enhanced chemiluminescence method (Amersham). Under nonreducing conditions, no signal for β_1-integrin was detected, suggesting that the antigenic epitope was not recognized; also, the molecular weight of α_3-integrin increased slightly as expected (reference 63 and data not shown).

To detect α_1-integrin, biotin labeling of cell surface proteins was performed (52). Briefly, cells were washed in PBS followed by borate buffer (50 mM sodium borate, 150 mM NaCl [pH 8.0]) and incubated with 100 μg of D-biotinoyl-ε-aminocapronic acid-*N*-hydroxysuccinimide ester (Boehringer Mannheim)/ml of borate buffer for 30 min at room temperature. Labeled cells were then collected from the plates in Tris buffer (50 mM Tris, 150 mM NaCl [pH 8.0]), centrifuged briefly, and washed twice in Tris buffer. The cells were then lysed in modified RIPA buffer on ice, the lysates were cleared, and protein was measured from the supernatants as described above. Lysates containing 2 mg of total protein were incubated with protein A-Sepharose beads (Pharmacia) passified with anti-mouse immunoglobulin G (Cappel) for 2 h at 4°C and then centrifuged to clarify the lysates. A 3-μl volume of 3A3 MAb (anti-α_1-integrin MAb provided by David Turner, State University of New York, Syracuse, N.Y.) and anti-mouse immunoglobulin G bound to protein A-Sepharose beads (30 μl packed volume) were then added to each lysate. The bound proteins were immunoprecipitated and resolved by SDS-PAGE (10% polyacrylamide), and biotinylated α_1-integrins were detected with horseradish peroxidase-conjugated streptavidin (Amersham).

Immunofluorescence labeling. PC12 or v-Crk-expressing cells were plated on poly-L-lysine-coated glass coverslips in serum-containing medium. At 24 h after plating, the cells were serum starved for 3 h to sensitize them for the serum response and then serum was reintroduced to the medium for 3 h. The cells were then washed in PBS and fixed in 3% paraformaldehyde in 0.9 mM $CaCl_2$- and 0.5 mM $MgCl_2$-containing PBS for 20 min at room temperature. Cell membranes were permeabilized by incubation of cells in 0.2% Triton X-100–1% blocking (horse or goat) serum in PBS for 15 min. Glass coverslips were then placed upside down on 150-μl droplets of various dilutions of primary antibodies in PBS containing 0.2% Triton X-100 and 0.1% blocking serum pipetted on Parafilm. After a 1-h incubation, coverslips were washed three times in PBS, blocked in PBS containing 0.2% Triton X-100 and 5% blocking serum, and placed for 1 h onto droplets of 1/100-diluted fluorescein isothiocyanate-conjugated anti-mouse antibodies or anti-rabbit antibodies (Vector Labs) and 0.5 μg of tetramethylrhodamine-5-isothiocyanate-conjugated phalloidin (Sigma) in PBS containing 0.2% Triton X-100 and 0.1% blocking serum. The cells were then washed four times in PBS for 10 min and once in deionized H_2O for 5 min and mounted on glass slides with Gelvatol. Staining was detected with a Zeiss Axiovert 100 microscope equipped with a plan-Neofluar objective (100×, 1.3 numerical aperture), and photographs were taken with Kodak Elite 400 film. In some experiments, glass coverslips were coated with 5 μg of fibronectin (Boehringer Mannheim) per cm^2, 1 μg of laminin (Sigma) per cm^2, 8 μg of collagen type I (Sigma) per cm^2, 10 μg of collagen type IV (GIBCO) per ml, and 33 μg of vitronectin (Calbiochem) per ml. Also, to overcome desensitization and test if the adhesions would acquire a more mature phenotype with thicker actin cables, we serum starved cells plated on vitronectin for 12 h (hence downregulating Rho activity) and then treated them with 1 μM LPA or serum (15%) for 3 h before performing immunofluorescence labeling. We did not detect any change in the form of adhesions generated under these conditions compared to those formed in cells maintained in serum.

Analysis of apoptosis. Native PC12 cells or v-Crk-expressing flat cells were cultured as above in 12-well plates, and triplicate plates were seeded with each cell line. Triplicate plates were treated in the presence or absence of serum, after which viability was analyzed by the LIVE/DEAD Viability/Cytotoxicity kit (Molecular Probes no. L-3224). This kit contains a two-color fluorescence assay that measures (i) intracellular esterase activity (a sign of viability) via the enzymatic conversion of nonfluorescent cell-permeant calcein AM to the intensely green polyanionic calcein, which is retained in live cells, and (ii) plasma membrane integrity by means of ethidium homodimer, which enters damaged membranes (a sign of cytotoxicity) and undergoes a 40× enhancement of red fluorescence upon binding DNA. The withdrawal experiments were begun at least 24 h after plating and when cell confluency approached 70%. After serum withdrawal, the cells were gently washed with 5 μl of PBS containing 0.9 mM $MgCl_2$ and 0.5 mM $CaCl_2$, after which 800 μl of LIVE/DEAD assay reagent (containing 4 μM ethidium homodimer and 2 μM calcein AM in PBS) was added to each well. The cells were incubated for 30 min at 37°C, and the percentages of live and dead cells were obtained by counting more than 1,000 cells per well from several random fields with a conventional 485-nm fluorescein excitation filter.

RESULTS

v-Crk induction of lamellipodia and somal flattening in PC12 cells is RhoA dependent and requires SH2 and SH3 domains of v-Crk. LPA, a major component of serum, induces the generation of focal adhesions and stress fibers in quiescent fibroblasts by a mechanism that appears to be dependent on the activation of the low-molecular-weight GTPase RhoA (62). In neuronal cells, including rat pheochromocytoma (PC12) cells, LPA causes growth cone collapse and neurite retraction (33, 66, 72), while inhibition of RhoA by C3 toxin leads to neurite outgrowth (34, 55). Previously, we reported that PC12 cells expressing the v-Crk adapter protein display an accelerated velocity of neurite outgrowth when treated with NGF in low (3%) serum (22, 28). However, when these cells were maintained in high (15%) serum, most of the cells developed lamellipodia with ruffling along the edges and exhibited marked somal flattening (Fig. 1 and 2A, arrows). To examine these cells in more detail, we isolated an essentially pure population of v-Crk-expressing flat cells (surface area, 617 ± 42 μm^2 [mean ± standard error]) from original v-Crk-expressing clones (V15 and V1) by physically separating them from round cells (surface area, 107 ± 73 μm^2) by manual trituration (Fig. 1, compare panels B and C). These flat cells will be referred to as V15F (v-Crk clone 15 flattened) throughout the paper. Similar results were observed with v-Crk clone V1, although unless otherwise indicated, only results from V15F cells are shown. Lamellipodium formation and somal flattening were dependent on the presence of serum (15%), since V15F cells readily reverted to the round phenotype when serum was withdrawn (Fig. 1A and Fig. 2B). The mean surface area of flat cells after serum withdrawal (137 ± 7 μm^2) was significantly different from the value obtained in serum (*t* test, $P < 0.001$). Flattening could also be induced upon treatment of cells with 1 μM LPA for 3 h in the absence of serum (Fig. 2D), which results in activation of Rho in PC12 cells (71). Treatment of V15F cells with 100 μg of C3 toxin per ml to block Rho activation, in contrast, prevented flattening in serum-containing medium (Fig. 2C) or by LPA (data not shown), suggesting that this effect is mediated by Rho. Moreover, as shown in Fig. 2C, C3 toxin treatment resulted in the formation of short neurite-like processes, although such neurite outgrowth was considerably less pronounced than in cells treated with NGF (not shown).

Previously, we have shown that v-Crk binds stably to the tyrosine-phosphorylated focal adhesion proteins paxillin and $p130^{cas}$ through its SH2 domain and to guanine nucleotide

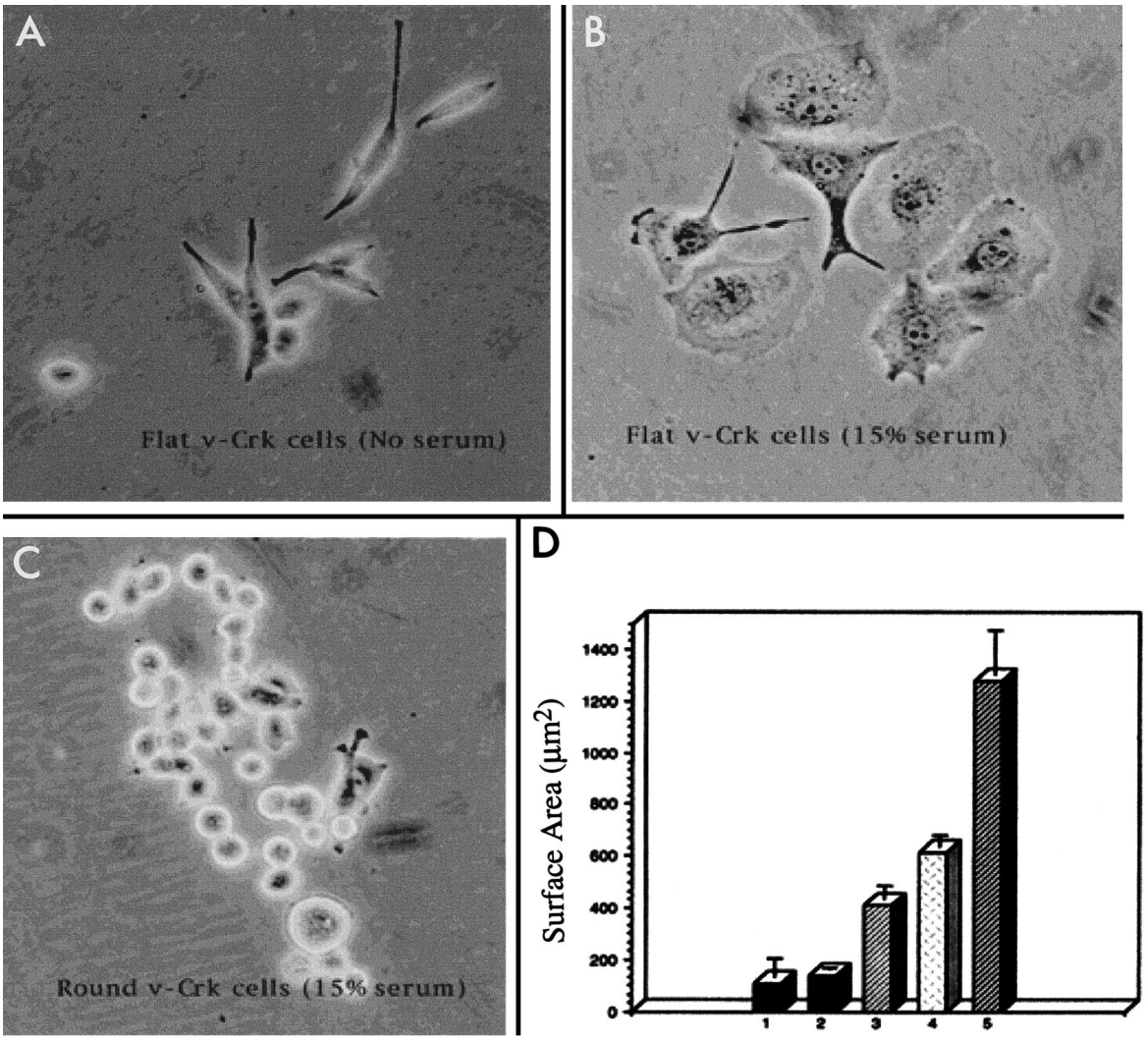

FIG. 1. Quantitative changes in the surface area of v-Crk-expressing cells in the presence and absence of serum and upon treatment with LPA or NGF. (B) When maintained in 15% serum-containing medium, the majority of v-Crk-expressing cells became flattened. (C) These cells were separated from the minor subset of cells that remained round in serum-containing medium, as described in the text. (A) When serum was withdrawn, the flattened v-Crk cells reverted to the round phenotype. (D) Bar graphs show the changes in mean surface areas of cells under various treatment conditions. The standard errors are also shown. The surface areas were measured by scanning photographs of random fields of cells and measuring the scanned images of individual cells on each photograph as described in Materials and Methods. (Bar 1) v-Crk cells that remained round in 15% serum; surface area, 107 + 73 μm^2 ($n = 51$). (Bar 2) Flat v-Crk cells in medium without serum; mean surface area, 137 + 7 μm^2 ($n = 40$). (Bar 3) Flat v-Crk cells that were maintained in the absence of serum and later treated with 1 μm LPA; mean surface area, 411 + 50 μm^2 ($n = 46$). (Bar 4) Flat v-Crk cells in 15% serum-containing medium; mean surface area, 617 + 42 μm^2 ($n = 45$). (Bar 5) Flat v-Crk cells maintained in 15% serum and then treated with 100 ng of NGF per ml for 5 days; mean surface area, 1,276 + 175 μm^2 ($n = 52$). The differences between mean surface areas of round versus flat v-Crk cells in 15% serum (t test, $P < 0.001$), flat v-Crk cells in the absence versus the presence of 15% serum (t test, $P < 0.001$), flat v-Crk cells in the absence of serum versus after LPA treatment (t test, $P < 0.001$), and v-Crk cells kept in serum versus after additional NGF treatment (t test, $P < 0.001$) were significant.

exchange factors (GNEFs) SOS1 and C3G through its SH3 domain (6) and, in doing so, may couple tyrosine kinase cascades to small GTPases in the neuronal cytoskeleton. To investigate whether lamellipodium formation was dependent upon SH2- or SH3-mediated pathways, we examined LPA-induced cell flattening in PC12 cells overexpressing SH2 or SH3 domain mutants of v-Crk. However, to first verify that these mutants were functionally inactive, we examined the binding of the SH2 mutants to tyrosine-phosphorylated paxillin and the binding of the SH3 mutants to a proline-rich peptide derived from C3G, since these proteins represent high-affinity Crk SH2- and SH3-binding proteins, respectively (6, 37) (Fig. 3). To determine whether R273N–v-Crk (SH2 mutant) perturbed the binding to tyrosine-phosphorylated paxillin, detergent lysates of v-Crk-expressing PC12 cells, R273N–v-Crk, and the linker insertion D386DRHAD–v-Crk were immunoprecipitated with anti-Gag antibodies and subjected to Western blotting with antipaxillin (Fig. 3A). In contrast to wild-type v-Crk and D386DRHAD–v-Crk, the R273N–v-Crk mutant was completely defective in its ability to coprecipitate paxillin, indicating a general defect in binding to a tyrosine-phosphorylated substrate.

To determine if the linker insertion mutation in the v-Crk SH3 domain impaired its binding to proline-rich sequences, we generated a GST–wild-type v-Crk SH3 domain and a GST–D386DRHAD–v-Crk SH3 domain after cloning into pGEX2TK, a vector which, in addition to producing a GST fusion, contains a cyclic AMP-dependent protein kinase phos-

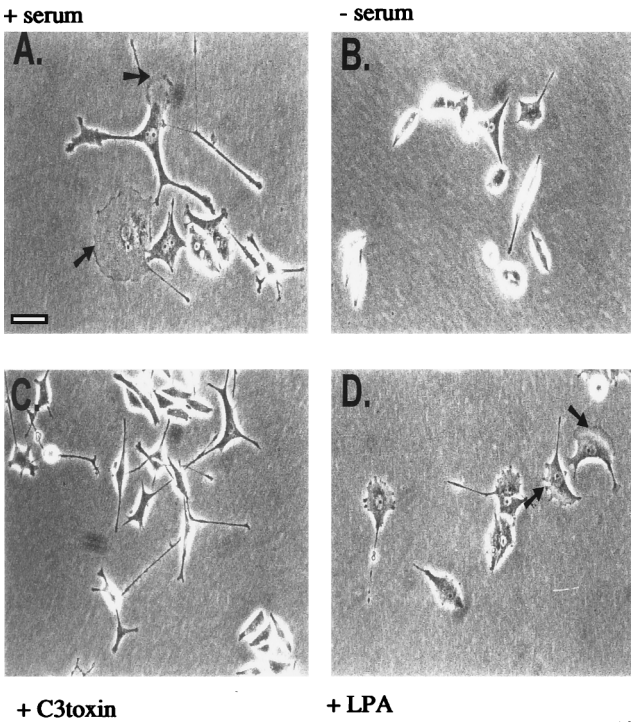

FIG. 2. v-Crk causes serum-induced cell flattening and lamellipodium formation in PC12 cells through the activation of Rho. v-Crk-expressing PC12 cells were grown in the presence (A and C) or absence (B and D) of 15% serum-containing medium. (A) Representative shape changes of PC12 cells expressing v-Crk when cultured in 15% serum. Cells flatten out and grow lamellipodia along their edges (arrows). (B) When cells are serum starved for 12 h, no flat cells are observed. (C) Cells maintained in 15% serum were treated with 100 μg of C3 exoenzyme per ml for 12 h. (D) Cells were maintained in serum-free medium for 12 h and then treated with 1 μM LPA for 3 h. Magnification, ×26.5. Bar, 50 μm.

phorylation site between the GST and the SH3 domain, enabling fusion proteins to be labeled to high specific activity (see Materials and Methods). To quantify the binding of GST-SH3 fusion proteins to proline-rich sequences, GST, GST-C3G CB1 (SPPPALPPK**K**RG), and GST-C3G K10L (SPPPALPPK**L**RG) were electrophoretically resolved, transferred to Immobilon, and incubated with either [^{32}P]GST, [^{32}P]GST–wild-type v-Crk SH3, or [^{32}P]D386DRHAD–v-Crk in an SH3 overlay assay. As shown in Fig. 3B, the insertional mutation within the Crk SH3 domain decreased its binding to the C3G peptide by more than 99%, indicating a total-loss-of-function mutation by this criterion. Given the fact that v-Crk SH2 and SH3 mutants were completely defective in binding their physiologically relevant proteins, we next compared the response of PC12 cells expressing these mutants to LPA (Fig. 3C). In contrast to results obtained with wild-type v-Crk PC12 cells (Fig. 2D), no cell flattening was induced in either mutant cell by treatment with LPA. Also, no cell flattening occurred when the cells were maintained in 15% serum (data not shown), suggesting that both the SH2 and SH3 domains of v-Crk are essential for the LPA- and serum-induced cell flattening. Moreover, consistent with previous results (33), LPA treatment of native PC12 cells resulted in complete rounding (Fig. 3C, panels i and iv).

v-Crk-expressing PC12 cells display isotropic growth with broadened lamellipodia after NGF treatment unless Rho activity is downregulated by serum withdrawal. To investigate the relationship between neurite elongation and lamellipodium formation, V15F cells were maintained in 15% serum and treated continuously with 100 ng of NGF per ml for 5 days (Fig. 4). In contrast to native PC12 cells, which grew long, branching neurites with well-developed growth cones in the presence of NGF (Fig. 4A), V15F cells grew broadened lamellipodia after NGF treatment (Fig. 4E and F, arrowheads). This NGF-induced isotropic growth of V15F cells was evident as a twofold increase in the mean surface area of the cells (Fig. 1D, compare histograms 4 and 5). Consistent with results in Fig. 3, neither D386DRHAD–v-Crk nor R273N–v-Crk cells exhibited somal flattening in NGF and 15% serum, although their responses to NGF were quite different (Fig. 4B and C). Thus, while R273N–v-Crk cells were defective in neurite elongation, SH3 mutants appeared to be equivalent to wild-type PC12 cells in their morphological appearance and velocity of differentiation. In contrast, when V15F cells were serum starved for 12 h before and during NGF treatment, their somas rounded and the cells extended long neurites (Fig. 4D). Consistent with previous results, the growth rate of these neurites was initially much higher than that of neurites extended from wild-type PC12 cells (reference 70 and data not shown). These data suggest that NGF-induced neuritogenic signals cannot be processed properly in flat-phenotype V15 cells unless Rho signaling is downregulated by serum withdrawal.

The Rho effector kinases, PI(4)P5-kinase and p160^{ROCK}, but not the Rac/Cdc42 effector kinases, PAK and S6 kinase, are activated by v-Crk. Among proteins that bind Rho, PI(4)P5-kinase (11) and p160^{ROCK} (Rho-associated coiled-coil-containing protein kinase) are activated by the GTP-bound form of Rho (31, 42, 50). To assess whether v-Crk modulates the activities of these Rho effectors, we measured the production of PIP_2 in v-Crk-expressing cells as a product of PI(4)P5-kinase (Fig. 5). Analysis of the total PIP_2 level revealed that it was increased about 1.6-fold in V15F cells maintained in 15% serum compared to levels found in wild-type cells. HPLC analysis of extracted lipids from V15F cells with respect to known standards of [^{3}H]PI(4)P, [^{3}H]PI(4,5)P_2, and [^{3}H]PI(3,4)P_2 revealed that v-Crk selectively elevated PI(4,5)P_2 levels whereas PI(3,4)P_2 was undetectable under these conditions (data not shown). These data support a role for v-Crk in Rho activation since GTP-bound recombinant Rho has been shown to bind PIP5-kinase, resulting in the selective production of PI(4,5)P_2 (11). Interestingly, in R273N–v-Crk- and D386DRHAD–v-Crk-expressing cells, the levels of PI(4,5)P_2 were approximately 47 and 67% of control values, respectively. These results suggest that basal levels of PI(4,5)P_2 are increased in the presence of wild type v-Crk and that the SH2 and SH3 mutants of v-Crk partially inhibit its production.

To directly test the effect of v-Crk on p160^{ROCK} activation, we used a transient-transfection assay whereby an expression vector encoding *myc*-tagged ROCK (pCMX-myc*ROCK*) was cotransfected with an expression vector for v-*crk* (pMEXneo-v-*crk*) into 293T cells. As a positive control for p160^{ROCK} activation, cells were cotransfected with pCMX-myc*ROCK* and pcEXV-*V14rhoA*, which encodes the constitutively active form of RhoA. After 24 h of incubation, the cells were lysed and immunoprecipitated with anti-Myc MAbs to quantify p160^{ROCK} activity in a kinase assay with histone H1 as the substrate. Figure 6A and B show two independent experiments demonstrating that when v-Crk was expressed, p160^{ROCK} activity was increased to levels similar to those seen after cotransfection of pcEXV-*V14rhoA*, suggesting that v-Crk lies upstream of Rho with respect to p160^{ROCK} activation. This level of p160^{ROCK} activation was quantitatively similar to the magnitude of activation reported previously after transient transfection of V14RhoA with p160^{ROCK} in COS cells (31). Moreover, as a control to show that v-Crk activation of p160^{ROCK} was Rho

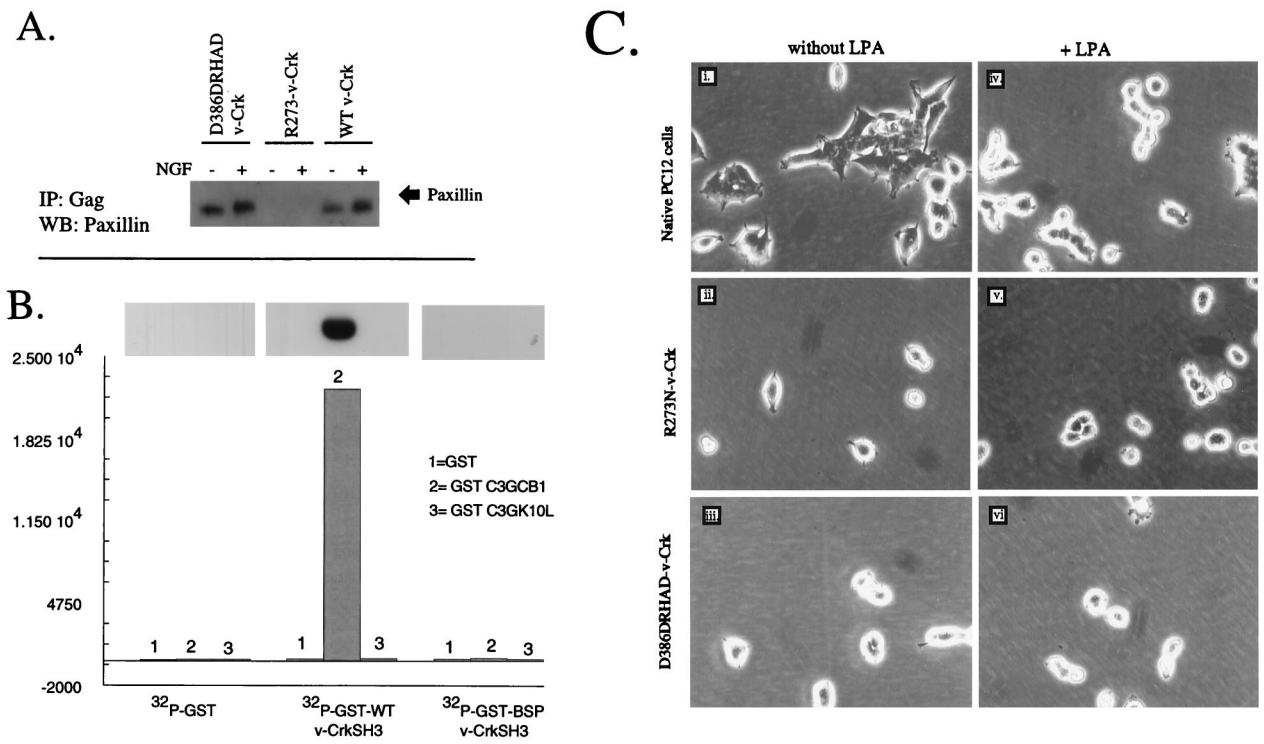

FIG. 3. Serum- and LPA-induced cell flattening is blocked by mutation in the v-Crk SH2 or SH3 domain. (A) R273N–v-Crk (SH2 mutant) is defective in binding tyrosine-phosphorylated paxillin. D386DRHAD–v-Crk, R273N–v-Crk, or wild-type (WT) v-Crk-expressing cells were kept in the presence or absence of NGF, and the resulting detergent lysates were immunoprecipitated with anti-Gag antibodies and subjected to Western blotting with antipaxillin MAb (arrow). (B) Linker insertion mutations in the Crk SH3 domain disrupt binding to proline-rich peptides derived from the Crk-binding region of C3G. GST or GST fusion proteins containing either wild-type v-Crk SH3 or D386DRHAD SH3 domains were labeled with [^{32}P]orthophosphate (see Materials and Methods). To quantify the binding of the ^{32}P-labeled GST proteins to C3G-derived peptides, 3.5 μg of GST (lanes 1), GST-C3GCB1 (SPPPALPPK**K**RG) (lanes 2), or GST-C3GK10L (SPPPALPPK**L**RG) (lanes 3) was electrophoretically resolved in a 13% acrylamide gel and transferred to Immobilon P, and membrane strips were incubated with [^{32}P]GST, [^{32}P]GST–v-Crk SH3, or [^{32}P]GST–D386DRHAD–v-Crk SH3 overnight at 4°C. After being washed, the filters were exposed to X-ray film (autoradiogram) or excised and counted in a β-counter (histograms). (C) Morphological responses of cells expressing v-Crk mutants towards LPA. Native PC12 cells (panels i and iv), R273N–v-Crk cells (panels ii and v), or D386DRHAD–v-Crk cells (panels iii and vi) were grown in serum-free medium for 12 h (panels i to iii) and then treated with 1 μM LPA for 3 h (panels iv to vi). Similar results were obtained with serum (not shown). BSP v-CrkSH3 is th esame as D386DRHAD–v-CrkSH3. The structures and positions of SH2 and SH3 mutations are indicated. Magnification, ×32.

dependent, cells transfected with v-Crk and mycROCK were cotransfected with either pEXV-N19RhoA or pEXV-N17Rac-1, which encode dominant negative forms of Rho and Rac, respectively (Fig. 6C). While v-Crk-mediated activation of p160^{ROCK} was strongly suppressed after transfection with N19RhoA, there was little or no inhibition of p160^{ROCK} activation by v-Crk in the presence of N17Rac-1.

In contrast to Rho, GTP-bound Rac and Cdc42 bind to and activate the serine/threonine kinases PAK (49) and S6 kinase (12). To determine whether v-Crk plays a role in activation of Rac/Cdc42-dependent protein kinases, PC12 cells and various v-Crk-expressing PC12 cells were maintained in low serum for 12 h and then stimulated with 15% serum or 15% serum plus 50 ng of NGF per ml for 30 min. As shown in Fig. 7, the kinase activities of cellular PAK65 (Fig. 7A) and S6 kinase (Fig. 7B) were not significantly increased upon serum or NGF addition, nor did v-Crk appear to hyperactivate their activities compared to control cells. Further, to demonstrate that v-Crk did not stimulate Rac/Cdc42-dependent kinases under conditions similar to those under which it activated p160^{ROCK}, 293T cells were also transiently cotransfected with vector DNA or pMEX–v-*crk* and an expression vector encoding hemagglutinin (HA)-tagged PAK (pJ3H-*PAK1*) (Fig. 7C). In contrast to PAK activation by V12Rac1 (a positive control for this experiment) and consistent with the results obtained with cellular PAK, there was no observable activation of transfected PAK by v-Crk. In contrast to PAK and S6 kinase, serum stimulation of normal PC12 cells did result in the activation of cellular JNK, and this appeared to be enhanced in V15F cells (Fig. 7D). Interestingly, the serum-induced JNK activation was almost completely abolished in PC12 cells expressing the SH3 mutant of v-Crk (D386DRHAD–v-Crk), suggesting that it may have a dominant negative effect in the JNK pathway. It is noteworthy that D386DHRAD–v-Crk did not decrease PAK or S6 kinase activities relative to the control levels, and this further suggests that the v-Crk- or serum-induced activation of JNK may not result from a Rac/Cdc42-dependent pathway in PC12 cells.

v-Crk induces stress fibers and focal adhesions at the cell periphery in response to serum in PC12 cells. In nonneuronal cells, microinjection of an activated form of Rho or overactivation of p160^{ROCK} promotes actin stress fiber and focal adhesion formation (42, 62). Neuronal cells, including PC12 cells, rarely contain focal adhesions. Moreover, activation of Rho results in retraction of neurites and cell rounding in NGF-treated PC12 cells (33). Since the phenotypic response of v-Crk cells to LPA or serum was reversed compared to that of wild-type cells, we investigated the presence of focal adhesions in these cells by immunofluorescence staining with antibodies against focal adhesion proteins. Neither PC12 cells nor V15F cells attached well to substratum in serum-deficient medium,

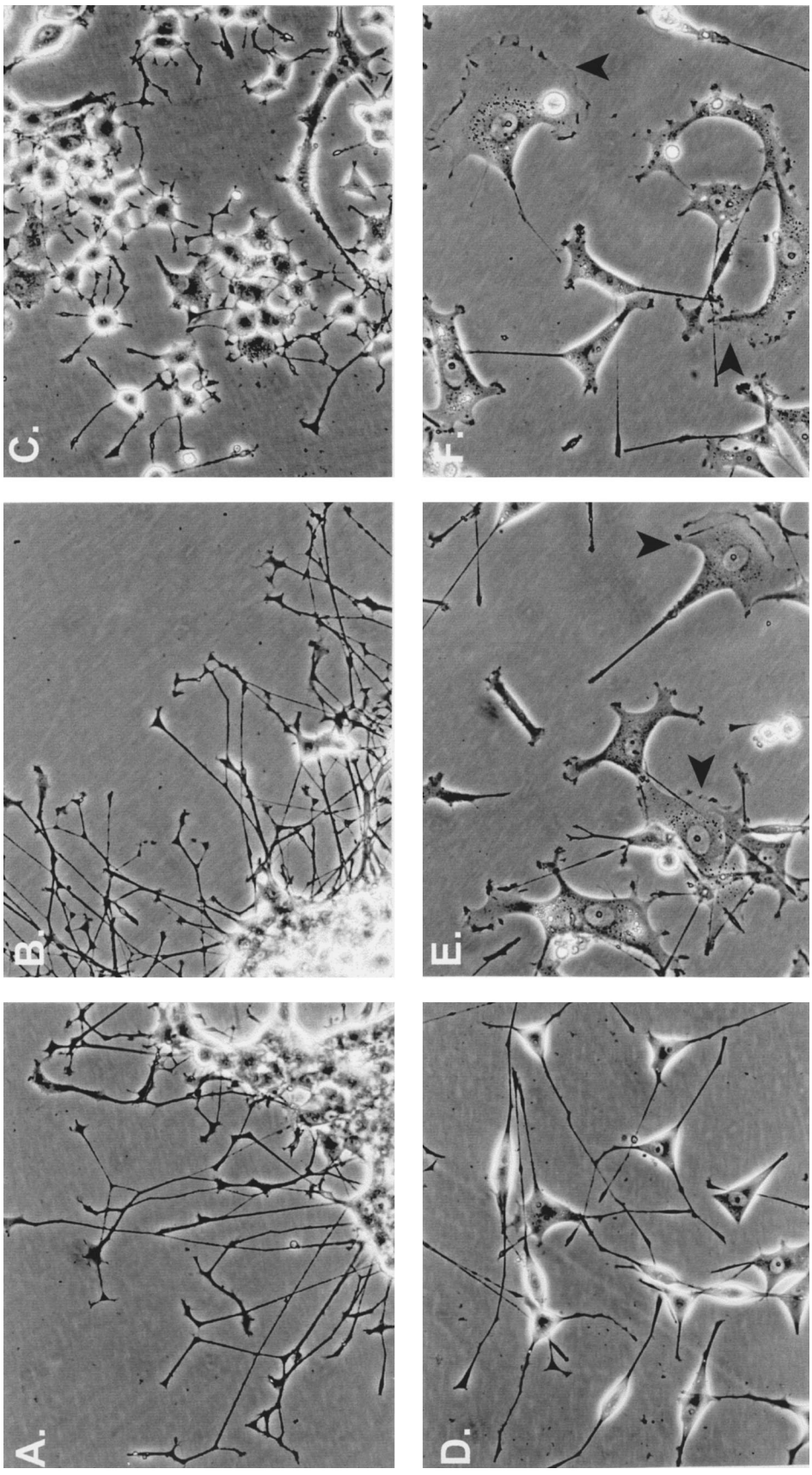

FIG. 4. LPA and serum antagonize the neurite-promoting effects of v-Crk unless serum is withdrawn. PC12 cells (A), D386DRHAD–v-Crk cells (B), R273N–v-Crk cells (C), or v-Crk cells (E and F) were cultured for 5 days in 15% serum containing NGF (100 ng/ml). v-Crk PC12 cells exhibiting broadened lamellipodia and flattening in panels E and F are indicated by solid arrows. In panel D, serum was removed from v-Crk-expressing cells for 12 h and the cells were cultured in serum-free medium containing 100 ng of NGF per ml. Note the absence of somal flattening in these cells (compare panel D with panels E and F).

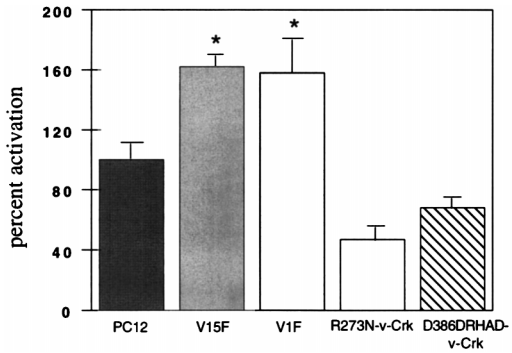

FIG. 5. PI(4,5)P_2 production in PC12 cells expressing v-Crk and v-Crk mutants. Native PC12 cells, v-Crk cells (clones V15F and V1F), R273N–v-Crk cells, or D386DRHAD–v-Crk cells were maintained in 15% serum, after which they were briefly starved and incubated overnight with 20 μCi of [^{32}P]orthophosphate. Extracts were prepared from adherent cells and normalized for cellular protein, and the resulting radiolabeled lipids were subjected to TLC. ^{32}P-labeled PIP_2 was deacylated and quantified with a PhosphorImager. Values were normalized to the value in native PC12 cells (designated 100%) and are expressed as the mean and standard error ($P < 0.05$ between V15F and V1F and native cells, indicated by asterisk) of four independent experiments. HPLC analysis on extracted lipids demonstrated that only PI(4,5)P_2, and not PI(3,4)P_2, was produced in these cells.

since probably both serum-related factors and extracellular matrix are required for adhesion complexes to form (29). Thus, PC12 and V15F cells were plated on poly-L-lysine-coated glass coverslips in the presence of serum which contains fibronectin and vitronectin, as well as serum-related factors such as LPA. After overnight incubation, the cells were stained with antibodies against the focal adhesion proteins paxillin and vinculin as well as a battery of anti-integrin-specific antibodies (Fig. 8 and data not shown). In all experiments, the cells were counterstained with rhodamine-conjugated phalloidin to detect F-actin. Interestingly, in V15F cells, vinculin and paxillin were localized in dash-like adhesion complexes (Fig. 8C and E) that were clearly associated with actin cables which either crossed the whole cytoplasm or formed circular cables around the cell periphery (compare Fig. 8C and D, and compare Fig. 8E and F). In fact, when these immunofluorescent scans were merged to identify points of colocalization, focal adhesions appeared yellow, indicating extensive colocalization of vinculin and paxillin with actin microfilaments (Fig. 8G and H). In contrast to V15F cells, vinculin or paxillin staining showed no discernible dash-like complex formation in native PC12 cells and actin staining was diffuse within the cytoplasm of these cells (Fig. 8A and B). An important distinction, however, between focal adhesion staining observed in fibroblasts and the adhesions in V15F cells was that the latter were preferentially localized to the cell periphery and the actin cables that associated with them were considerably thinner. These adhesion complexes are similar to the transitory-type focal adhesions or "immature" focal adhesions described by Bershadsky et al. (5). Staining with antibodies against Gag (to detect v-Crk) also revealed that Crk localized to similar complexes (data not shown), consistent with previous results obtained with fibroblasts (54).

To investigate whether v-Crk expression resulted in a redistribution of integrins into focal adhesions, we surveyed a variety of anti-integrin antibodies, including anti-α_1, anti-α_3, anti-α_v, and anti-β_1, in the V15F cells. In contrast to the well-demarcated vinculin and paxillin staining observed in focal adhesions, α_1, α_3, or α_v staining was predominantly punctate and did not localize to focal adhesions (not shown). In fact, staining of β_1-integrin, which represents a major integrin in PC12 cells (15), was observed in punctate complexes at the periphery of lamellipodia. We did not detect any actin fibers associating with these punctate adhesions, suggesting that β_1-integrin may not be the primary integrin utilized by v-Crk. These results raise the possibility that v-Crk regulates novel integrin pathways during focal adhesion biogenesis. Since it has been reported that the type of matrix determines the distribution of distinct integrins into focal contacts (16), we also

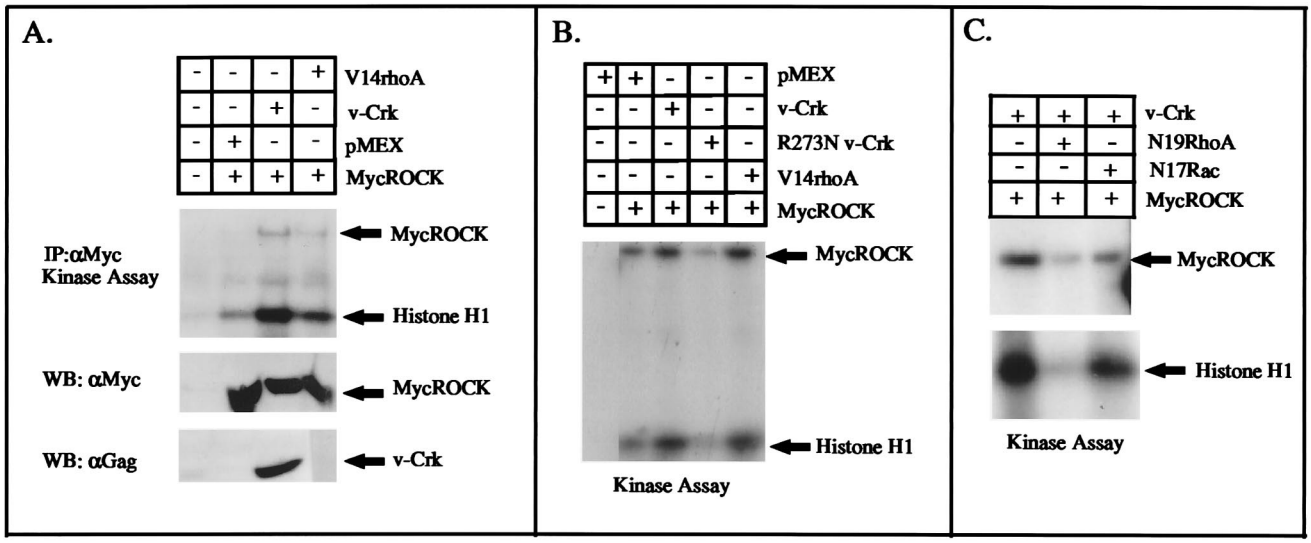

FIG. 6. v-Crk activates p160^{ROCK} by transient transfection into 293T cells. (A) 293T cells were transiently cotransfected by the calcium phosphate method with 2 μg of pCMX-myc-tagged ROCK (lanes 2 to 4) and either 2 μg of pMEXneo (control, lane 2), pMEXneo–v-*crk* (lane 3), or activated pcEXV-*V14rhoA* (lane 4) for 3 h. After an additional 36 h in 15% serum, the cells were washed and immunoprecipitated with anti-Myc MAb. In the top panel, the level of p160^{ROCK} activity was determined in an in vitro kinase assay with 5 μg of histone H1 as a substrate. The expression levels of myc-p160^{ROCK} and v-Crk, determined by Western blotting, are shown in the respective bottom panels. (B) A replicate experiment, except that cells were also transfected with 2 μg of pMEXneo–R273N–v-*crk* plasmid DNA. (C) Effects of dominant negative Rho or Rac on the v-Crk-induced activation of MycROCK. Transfections were performed as above, except that 2 μg of pEXV-N19rhoA (lane 2) or pEXV-N17rac1 (lane 3) was used as the control for Rho specificity.

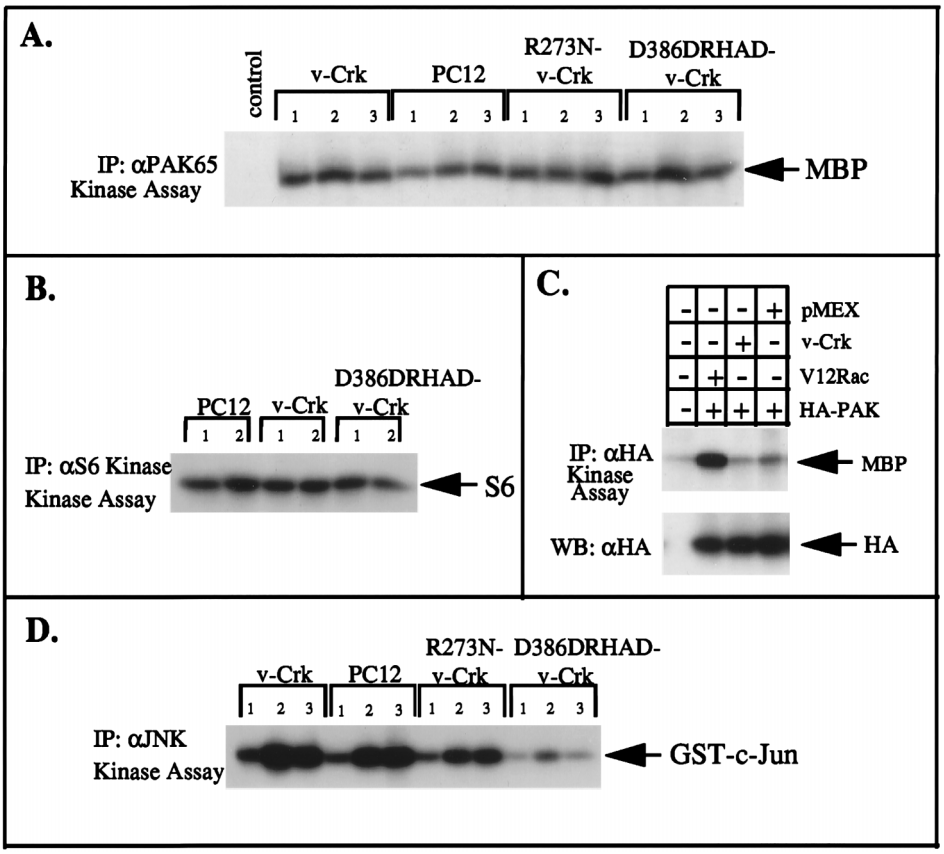

FIG. 7. The Rac/Cdc42-activated protein kinases PAK and S6 kinase are not hyperactivated by v-Crk. (A and B) Native, R273N–v-Crk-expressing, D386DHRAD–v-Crk-expressing, or v-Crk-expressing PC12 cells were serum starved for 12 h (lanes 1) and then stimulated with 15% serum (lanes 2) or 15% serum plus 50 ng of NGF per ml (lanes 3) for an additional 30 min. The cells were washed, detergent lysates were prepared, and 500 μg of total cellular protein was immunoprecipitated with either anti-PAK65 polyclonal antibody (A) or anti-S6 kinase polyclonal antibody (B). The kinase activity was determined after incorporation of ^{32}P into myelin basic protein (MBP) or S6 proteins, respectively (indicated by arrows). (C) 293T cells were transiently transfected as described in the legend to Fig. 6A, except that 2 μg of pJ3H-PAK DNA and 2 μg of either pEXV-V12rac1 (lane 2), pMex-v-Crk (lane 3), or pMEXneo control (lane 4) were used. The cells were lysed and immunoprecipitated with anti-HA antibodies, and kinase activity was measured with 5 μg of myelin basic protein as the substrate (arrow). The expression of HA-PAK by using anti-HA antibody is indicated in the bottom panel (arrow). (D) Activation of cellular JNK by v-Crk and mutant v-Crk. PC12 cells and wild-type or mutant v-Crk PC12 cells were treated as above and immunoprecipitated with anti-JNK antibodies. Kinase activity was measured after incorporation of ^{32}P into the GST–c-Jun 1-79 substrate (arrow).

examined whether changing the extracellular matrix type to vitronectin, fibronectin, collagen types I and IV, or laminin would affect the pattern of staining of adhesion complex proteins and actin in V15F cells. However, no noticeable change in the staining of actin, integrins, or vinculin was detected on any of these matrices (data not shown).

v-Crk-expressing cells contain an increased level of FAK, which is constitutively active in adherent cells. During focal adhesion assembly, LPA or Rho activation causes tyrosine phosphorylation of several cytoskeletal proteins, including paxillin, p130^{cas}, and FAK (39, 65). To test whether v-Crk expression resulted in a modulation of FAK tyrosine phosphorylation, we immunoprecipitated FAK from lysates of native PC12 cells and V15F cells and tested for tyrosine phosphorylation by immunoblotting with an antiphosphotyrosine antibody. In contrast to native PC12 cells, in which no tyrosine phosphorylation of FAK could be detected, FAK was constitutively tyrosine phosphorylated in V15F cells (Fig. 9A, top panel). Moreover, when the immunoblots in Fig. 9A were stripped and reanalyzed for the levels of FAK by anti-FAK immunoblotting, the expression of FAK was found to be increased in V15F cells (Fig. 9A, bottom panel). To investigate whether FAK phosphorylation was dependent on cell adhesion, V15F cells were trypsinized and either replated on matrix for 4 h (Fig. 9B, lanes 2 and 3) or grown in suspension in the presence of serum for 4 h (Fig. 9B, lane 4). Tyrosine phosphorylation of FAK was strictly dependent on adhesion to matrix (Fig. 9B, compare lanes 2 and 4), although the level of FAK expression remained elevated (compare lanes 3 and 4 in the bottom panel). Similarly, when V15F cells were treated with C3 toxin for 12 or 24 h to cause cell rounding (Fig. 2C), FAK tyrosine phosphorylation was also abolished while the expression of FAK remained elevated (Fig. 9B, lanes 5 to 7). Since v-Crk expression caused an upregulation in the level of FAK, we postulated that a change in the level of adhesion proteins might explain the reversion of phenotypic response of v-Crk-expressing PC12 cells to LPA and serum. Therefore, we compared the expression of several cytoskeletal proteins and integrins in the phenotypically "flattened" v-Crk-expressing cells (V15F) to that in v-Crk-expressing cells that were phenotypically round (see Materials and Methods), as well as in mutant v-Crk-expressing cells and naive PC12 cells (Fig. 10). Indeed, the amount of FAK was increased in both round and flat v-Crk cells (Fig. 10, compare lanes 4 through 7 to lane 1). Also, the comparative levels in v-Crk cells correlated with their phenotype in serum, such that flattening was seen only in cells that contained higher

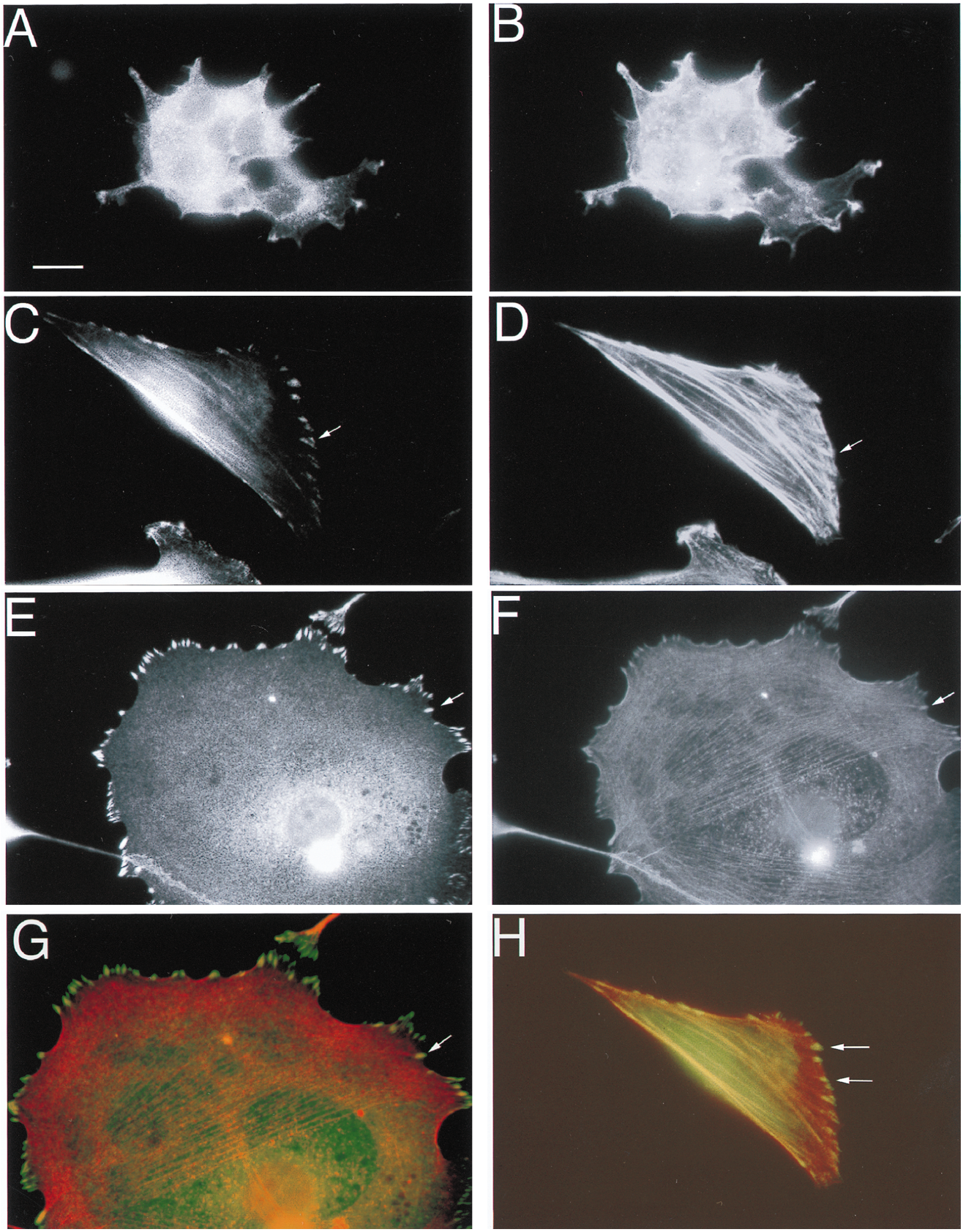

FIG. 8. v-Crk promotes the formation of stress fibers and focal adhesions that contain vinculin and paxillin. Native PC12 cells (A and B) or V15F cells (C to H) were cultured in 15% serum on poly(L-lysine)-coated glass coverslips. The cells were immunostained with antipaxillin (A and C) or antivinculin (E) antibodies and counterstained with rhodamine-conjugated phalloidin (B, D, and F) to detect actin microfilaments. Solid arrows demarcate areas of well-defined peripheral focal adhesions that end in stress fibers (compare the arrows in panels C and D and those in panels E and F). Panels G and H show merged composites of vinculin and actin (G) and paxillin and actin (H). Focal adhesions that stained yellow (arrows) indicate regions of colocalization. Magnification, ×91. Scale bar, 3.3 μm in panels A and B; 10 μm in panels C through H.

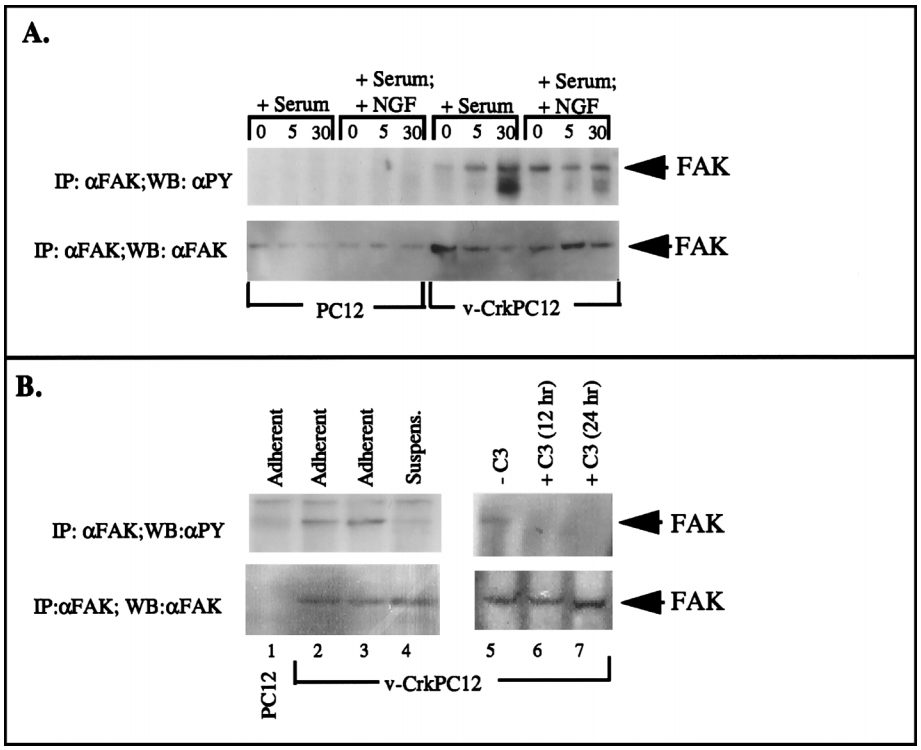

FIG. 9. v-Crk elevates the expression and tyrosine phosphorylation of FAK. (A) PC12 or V15F cells were maintained in low serum (3%) for 4 h and then stimulated with either 15% serum or 15% serum plus 100 ng of NGF per ml for 5 or 30 min. Lysates were normalized for cellular protein, immunoprecipitated with anti-FAK MAb, and subjected to Western blotting with anti-PY (top panel). In the bottom panel, the same blot was stripped and reprobed with anti-FAK antibody. The constitutive level of tyrosine phosphorylation in the presence of low serum probably reflects the fact that the cells were kept in low serum for only 4 h, at which time they were still predominantly flattened. (B) Tyrosine phosphorylation of FAK in V15F cells is dependent on cell adhesion and Rho activation (lanes 2 to 7). The cells were treated as in panel A, except in lane 4, where V15F cells were treated with EDTA and grown in suspension in spinner flasks with 15% serum for 4 h. In lanes 5 to 7, V15F cells were treated in the absence (lane 5) or presence (lanes 6 and 7) of C3 toxin for 12 or 24 h. The levels and tyrosine phosphorylation of FAK are indicated.

levels of FAK. In contrast, total Western blotting of native PC12 and SH2 and SH3 mutants did not show detectable levels of FAK expression (lanes 1 through 3). This suggests that expression of v-Crk in PC12 cells leads to upregulation of FAK in these cells and also that there is a threshold level of FAK within cells, below which the cells respond to serum by rounding up. In addition to FAK, V15F cells exhibited an increase in the expression level of paxillin, α_3-integrin, and a higher-molecular-weight form of β_1-integrin (Fig. 10) but not of other adhesion-related proteins such as vinculin, talin, and p130^{cas}. We did not detect any α_5-integrin in PC12 cells (data not shown), and α_1-integrin expression was unchanged in v-Crk PC12 cells (Fig. 10). These data suggest that v-Crk expression leads to increased levels of specific adhesion proteins in PC12 cells.

Expression of v-Crk confers resistance to apoptosis. Cells require anchorage to the substratum and the presence of growth factors for survival. However, overactivation in the signaling cascades initiated by either one of these factors can confer anchorage- or serum-independent growth. Recently, it has been reported that constitutively activated forms of FAK, which form, for example, by targeting FAK to plasma membranes, protect cells from a specific form of apoptosis called anoikis (19). To address whether the expression of v-Crk confers resistance to apoptosis in PC12 cells, we induced cell death by serum and growth factor withdrawal in V15F and PC12 cells (Fig. 11). By 36 h after serum withdrawal, about 50% of wild-type PC12 cells underwent apoptosis whereas more than 95% of the V15F cells remained alive. Similar results were obtained with other wild-type v-Crk-expressing clones (data not shown). Our results suggest that v-Crk can regulate survival signals and that ectopic expression of v-Crk renders PC12 cells resistant to apoptosis, probably via the upregulation and activation of FAK.

DISCUSSION

The Rho family of GTP-binding proteins regulates rearrangement of the actin cytoskeleton in many different cell types. In neuronal cells, including PC12 cells, the interplay between neurite extension and neurite retraction may be controlled in part by the relative activation of Rac/Cdc42 and Rho (45, 47). Activated Rac and Cdc42 are involved in maintaining growth cone structures such as lamellae and filopodia, thereby facilitating neurite elongation, while activation of Rho, for example by serum or LPA, induces cell rounding and inhibits neurite outgrowth by causing growth cone collapse (38). Evidence for this is supported by results obtained with *Drosophila* embryos, in which dominant negative Rac impairs axonal pathfinding in developing sensory neurons (44, 46). In this paper, we present evidence that the SH2/SH3 domain-containing protein v-Crk activates downstream effectors of Rho but not Rac or Cdc42 and reverses the cytoskeletal response of PC12 cells to LPA and serum by causing cell flattening. PC12 flattening as a result of v-Crk expression correlates with the formation of well-organized focal adhesions and stress fibers, reflecting increased PI(4,5)P_2 production and FAK activity and increased expression of FAK, paxillin, α_3-integrin, and a higher-molec-

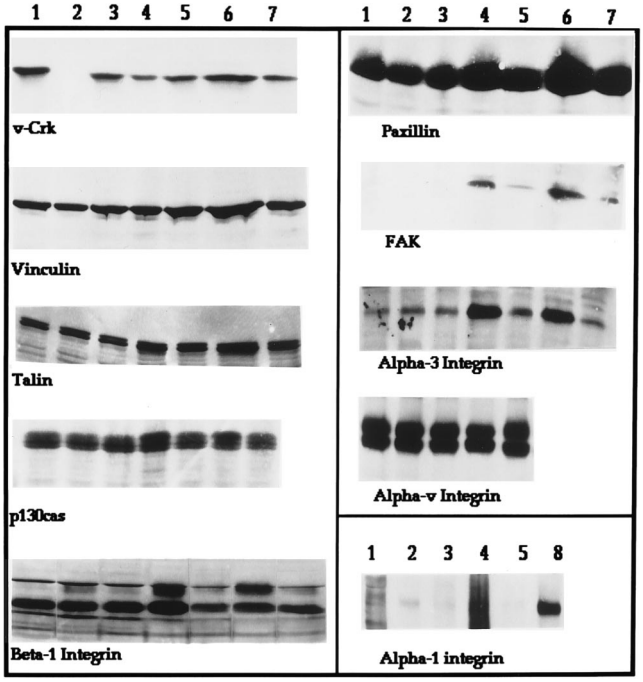

FIG. 10. The expression levels of FAK, paxillin, α_3-integrin, and a higher-molecular-weight form of β_1-integrin are selectively increased in v-Crk-expressing cells. D386DRHAD–v-Crk (lane 1), native PC12 cells (lane 2), R273N–v-Crk (lanes 3), and round or flat forms of two independent lines of v-Crk cells, V1 flat cells (lanes 4), V1 round cells (lanes 5), V15 flat cells (lanes 6), and V15 round cells (lanes 7), were maintained in 15% serum. Round cells were obtained by slight manual trituration of the cells, which lifted off the plate easily, leaving the flattened cells which contained focal adhesions still attached. After cell lysis, protein concentrations were normalized and 100 μg of total cellular protein was analyzed by SDS-PAGE and Western blotting with specific antibodies to Gag (v-Crk), vinculin, talin, $p130^{cas}$, β_1-integrin, paxillin, FAK, α_3-integrin, and α_v-integrin, as indicated. Expression of FAK was increased in both forms of v-Crk cells, although to a lesser degree in the round cells (compare lanes 4 and 6, and compare lanes 5 and 7). α_1-Integrin was detected after cell surface biotinylation followed by immunoprecipitation and immunoblotting with horseradish peroxidase-conjugated streptavidin. Although another strain of PC12 cells expressed α_1-integrin at high levels (lane 8), the PC12 cells used in this study as well as v-Crk and mutant v-Crk-expressing cells showed very low detectable levels of α_1-integrin.

ular-weight form of β_1-integrin in the cells. It is possible that in v-Crk-expressing PC12 cells higher levels of FAK and adhesion proteins permit cell flattening and focal adhesion formation in response to Rho activation, similar to that which occurs in fibroblasts, while in native PC12 cells Rho activation causes cell rounding, presumably due to below-threshold levels of FAK and adhesion-related proteins. Our results suggest that the composition of cytoskeleton-associated molecules in neuronal cells, as well as the relative activity of adhesion complex-related signaling molecules, determines the response of neurons to serum and growth factors. Moreover, our data support a role for v-Crk as an intrinsic determinant for the organization of adhesion complexes in PC12 cells.

The effects of LPA and serum on focal adhesion and stress fiber formation are mediated by Rho (62), although the exact signaling steps that lead to Rho activation downstream of LPA have not yet been elucidated. The conversion from the GDP-bound form of Rho to the GTP-bound form is regulated by two classes of protein factors: Rho GDI and GNEFs (25). In unstimulated cells, Rho GDI binds and prevents guanine nucleotide exchange on Rho as well as maintaining this GTPase in the cytoplasm (1, 7). Upon stimulation by serum or LPA, GNEFs, such as Dbl or Lbs, stimulate GTP exchange on Rho, which dissociates from Rho GDI and becomes translocated to the membrane fraction (7). A growing family of 15 or more proteins, including Ost, faciogenital dysplasia protein, Isc, Abr, Bcr, Tiam-1, and Vav, possess Dbl homology (DH) domains and may act as GNEFs for Rho family GTPases (10, 20). All of these proteins also contain pleckstrin homology domains, which bind to inositol phospholipids and are required for membrane targeting and guanine nucleotide exchange activity (79). The activities of GNEFs may also be modulated by tyrosine phosphorylation, since Lck, a member of the Src family of tyrosine kinases, can tyrosine phosphorylate and activate Vav, a GNEF for Rho GTPases (14, 24). It is not yet clear, however, whether tyrosine phosphorylation is used as a strategy for activation of other GNEFs for Rho family GTPases. Our results suggest that the activity of one of these upstream regulators of Rho, Rho GDI or a GNEF, is controlled by v-Crk. Previously, we have shown that v-Crk expression results in sustained growth factor-induced mitogen-activated protein kinase (MAPK) activity in PC12 cells (70) and that this effect is dependent on an intact SH3 domain of v-Crk. We have suggested that v-Crk binding to SOS, a GNEF for Ras, through its SH3 domain leads to increased activity of Ras and MAPK activation downstream of Ras. Through this domain, v-Crk also binds C3G, which was shown to be a GNEF for Rap-1 (23, 68). Results by Tanaka et al. have shown that C3G augments the v-Crk-induced activation of JNK and that this pathway leads to cellular transformation (69). It remains to be determined whether C3G plays any role in Rho activation or whether C3G overexpression induces flattening or stress fiber formation in our system. It is possible that v-Crk also binds a yet unknown GNEF for Rho and leads to sustained activation of Rho and its downstream effectors. However, to date, none of the cellular proteins that bind to the CrkSH3 domain, SOS, C3G, EPS15, DOCK180, Abl, or P13-kinase (6), contain DH domains, and thus none are obvious candidates for a direct Rho GNEF.

Tyrosine kinases were found to be required at signaling steps both upstream and downstream of Rho, since treatment of cells with a tyrosine kinase inhibitor, tryphostin, blocks Rho activation specifically at an upstream step (57). In contrast, another tyrosine kinase inhibitor, genistein, inhibits focal adhesion assembly and stress fiber formation downstream of activated Rho (61). Introduction of activated forms of Rho into cells results in increased tyrosine phosphorylation of several

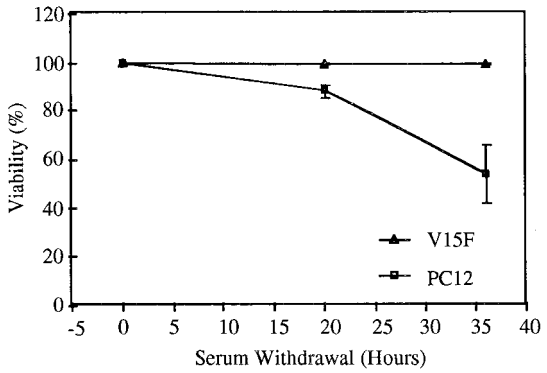

FIG. 11. v-Crk confers resistance to apoptosis during serum withdrawal. Native PC12 or V15F PC12 cells were cultured in 15% serum and transferred to serum-free medium for up to 36 h. Live versus dead cells were scored by a two-color fluorescence assay involving ethidium homodimer and calcein AM. Data show the mean and standard error for three independent experiments.

cytoskeletal proteins, such as paxillin, FAK, and p130^{cas} (18, 65). As suggested for focal adhesion assembly, this finding can be explained by Rho-induced acto-myosin contraction and resulting adhesion complex clustering (13). Clustering of integrin-bound complexes would bring tyrosine kinases within these complexes into close proximity and result in their *trans*-phosphorylation and activation. Currently, it is believed that GTP binding of Rho leads to acto-myosin contraction through activation of ROCKs, one of which phosphorylates and inactivates a myosin light-chain phosphatase (36). Increased phosphorylation of myosin light chain correlates with increased acto-myosin contraction and precedes the formation of stress fibers and focal adhesions (13). Also, it has recently been shown that overexpression of p160^{ROCK} can directly promote stress fiber formation and focal adhesion assembly in fibroblasts and HeLa cells (3, 32). Rho in its GTP-bound form also binds and activates a PIP5-kinase, resulting in increased production of PI(4,5)P_2 (60). PIP_2, in turn, removes barbed end-capping proteins from actin filament ends, allowing filament elongation and an increase in the level of polymerized actin (27). Also, by inducing a conformational change in vinculin, PIP_2 exposes binding sites for talin and actin on vinculin (21), further promoting actin-containing adhesion complex assembly. We found that the activation levels of p160^{ROCK} and a PIP5-kinase in v-Crk-expressing PC12 cells are increased simultaneously, suggesting that v-Crk may function to control both of these regulators of actin cytoskeleton downstream of Rho.

In *Saccaromyces cerevisiae*, a scaffolding protein, Ste5p, is important during the mating response to pheromones in linking the MAPK module which controls transcriptional activation to the actin cytoskeleton-regulatory module which controls polarized morphogenesis (41). Ste5p is suggested to spatially restrict these signaling components, which also play a role in pseudohyphal growth, providing specificity for the mating response. The two modules that are brought together by Ste5p comprise the Rho-like small GTPase Cdc42p, a GNEF for this GTPase, Cdc24p, as well as the Ste20p family of serine/threonine kinases, which are homologs of mammalian PAKs, an SH3-containing protein Bem1p, actin, and yeast MAPK homologs. It is possible that v-Crk serves an analogous scaffold function in mammalian cells to spatially link Rho-dependent actin signaling to the tyrosine kinase signaling during focal adhesion assembly, since the v-Crk SH2 domain binds substrates of the FAK and Src family of tyrosine kinases, paxillin, and p130^{cas}. Paxillin and p130^{cas} in turn bind other focal adhesion proteins, including FAK, vinculin, α-actinin, talin, and integrins (26, 53). Furthermore, we have recently shown that in fibroblasts, v-Crk potentiates phosphotyrosine-dependent signaling within focal adhesions, which could serve as nucleation sites for signaling proteins such as Grb2, Src, Nck, and PI(3)-kinase (64). In the presence of v-Crk, this cytoskeletal complex might therefore be placed in the proximity of regulators of actin, such as PIP(5)-kinase or p160^{ROCK}, which are controlled by Rho. In v-Crk-expressing PC12 cells, both vinculin and paxillin localize to focal adhesions that look similar to the transitory-type focal adhesions described by Bershadsky et al. in quail embryo fibroblasts (5). Although these adhesions are seen preferentially at the cell periphery and the associated actin fibers are thin, they are clearly distinct from focal complexes, which do not associate with actin fibers and are formed downstream of Rac activation.

We detected that expression of v-Crk leads to an increase in the amount of FAK protein expression in PC12 cells. This may be due to positive-feedback signals to the nucleus which originate from adhesion complexes; conversely, degradation of FAK may be slower in these cells. We are currently trying to distinguish between these two possibilities. Our results suggest that until a certain threshold level of FAK is reached, v-Crk-expressing PC12 cells do not acquire a flattened phenotype in serum. This phenotypic conversion also correlates with increased amounts of specific adhesion complex proteins such as paxillin, α_3-integrin, and a higher-molecular-weight form of β_1-integrin, although we do not know their precise role during cell flattening. Recent studies have shown that aggregation of FAK, by fusion to the ectodomain of CD2, causes constitutive activation and accelerates the spreading of MDCK cells on collagen (19). Activated FAK also confers resistance to a type of apoptosis called aniokis, which occurs when cells detach from extracellular matrix (30), and, as shown here, V15F cells that display upregulation of FAK are highly resistant to apoptosis during serum withdrawal. An interesting question is how two GTPase (Ras and Rho)-dependent signals are spatially and temporally coordinated at the level of v-Crk in PC12 cells, since both signaling cascades seem to be potentiated by this protein. Our previous work suggests that coupling of sustained Ras and MAPK activation to tyrosine kinase signals is critical for potentiated differentiation in v-Crk-expressing PC12 cells (70). However, facilitation of neurite elongation does not become obvious in V15F when these cells are stimulated with NGF; instead, a twofold isotropic enlargement in their mean surface area is observed. Once activation of Rho is suppressed by serum withdrawal or C3 toxin pretreatment, the cell soma becomes round and individual axons are formed in response to NGF. Also, the initial stage of axon formation and elongation is more rapid in these cells than in wild-type PC12 cells, as we described previously (28). Hence, in V15F cells, activation of Rho signals may counteract Ras-activated signals, which are required for NGF-induced differentiation. In contrast to wild-type PC12 cells, in which Rho activation blocks neurite outgrowth by inducing growth cone collapse, differentiation is masked in v-Crk cells by increased flattening after NGF treatment.

Our present assays did not determine which integrins are responsible for accumulation of these focal adhesions in v-Crk-expressing PC12 cells. Previously it was shown that the ligand specificities of integrins determine their distribution to focal adhesions (16). When the cells are plated on a specific extracellular matrix molecule, the integrin receptors specific for that molecule are seen to be driven into focal adhesions that form within these cells. Recently, it has been shown that a short sequence of the β subunit of the integrin dimer may determine substrate specificity and hence distribution to focal adhesions (67). In our assays, we could not detect any of the integrin subunits we tested within focal adhesions of v-Crk cells which were plated in fibronectin- and vitronectin-containing serum. Also, this result was not affected by plating cells on various other substrata. Previously, $\alpha_1\beta_1$- and $\alpha_3\beta_1$-integrins, which recognize different domains in laminin, were shown to be expressed in PC12 cells (73). Among these, $\alpha_1\beta_1$-integrin is variably expressed in different strains of PC12 cells, and its expression can be induced by NGF treatment (78). Indeed, in PC12 strains, which we used in this study and which were constructed to express v-Crk protein, $\alpha_1\beta_1$-integrin expression was much lower than in another PC12 strain (Fig. 10, compare lanes 2 and 8). We did not detect any increase in $\alpha_1\beta_1$-integrin levels in flat v-Crk cells. Immunofluorescent staining with MAb 3A3 (against the α_1 subunit) as well as with anti-β_1-integrin subunit antibody showed localization of β_1-integrins, including $\alpha_1\beta_1$-integrin, in small punctate adhesions along the cell periphery. Although an increase in $\alpha_3\beta_1$-integrin levels may be a prerequisite for the cell-flattening response to serum, we could not

detect $\alpha_3\beta_1$-integrin in focal adhesions even when cells were plated on laminin, suggesting that this integrin does not take part in the formation of these adhesions in v-Crk cells. We could not detect any $\alpha_5\beta_1$-integrin, which binds to fibronectin and was previously shown to localize to focal adhesions in fibroblasts, in PC12 cells. In V15F cells, α_v-integrin staining was seen within small, granular adhesion complexes throughout the ventral cell surface. Hence, our results suggest that a currently unidentified integrin may be involved in the formation of these focal adhesions in v-Crk cells.

In summary, we have presented evidence that v-Crk activates the Rho pathway in PC12 cells to induce stress fibers and focal adhesion biogenesis following serum or LPA stimulation. Formation of focal adhesions accompanies an upregulation in the expression of the focal adhesion proteins FAK and paxillin, as well as in the activation of adhesion complex-related kinases, suggesting that v-Crk may coordinate protein-protein interaction with focal adhesions. Future studies that identify the components of the v-Crk signaling pathway should shed light on the molecular mechanisms linking Rho-GTP to focal adhesion biogenesis.

ACKNOWLEDGMENTS

We thank Filipo Giancotti, David Turner, Louis Reichardt, and Alan Hall for reagents and helpful discussions during the course of this work. We also thank Alan Hall (University College, London, United Kingdom) for providing expression vectors encoding V12Rac1, V14RhoA, N17Rac1, and N19RhoA and Gary Bokoch (The Scripps Research Center, La Jolla, Calif.) for providing pJ3H-*PAK1* DNA. We thank Roman Burzynski, Rockefeller University media resource center, and Tan A. Ince for excellent technical assistance in the computerized reconstruction of the figures.

This work was supported by NIH grants to R.B.B. (NS30687), H.H. (CA44356), and J. A. W. (EY06454 and NS31728).

REFERENCES

1. **Adra, C. N., D. Manor, J. L. Ko, S. Zhu, T. Horiuchi, L. Van Aelst, R. A. Cerione, and B. Lim.** 1997. RhoGDIgamma: a GDI-dissociation inhibitor for Rho proteins with preferential expression in brain and pancreas. Proc. Natl. Acad. Sci. USA **94:**4279–4284.
2. **Altun-Gultekin, Z. F., and J. A. Wagner.** 1996. Src, ras, and rac mediate the migratory response elicited by NGF and PMA in PC12 cells. J. Neurosci. Res. **44:**308–327.
3. **Arraro, M., K. Chihara, K. Kimura, Y. Fukata, N. Nahamura, Y. Matsura, and K. Kaibuchi.** 1996. Formation of actin stress fibers and focal adhesions enhanced by rho-kinase. Science **275:**1308–1311.
4. **Barry, S. T., H. M. Flinn, M. J. Humphries, D. R. Critchley, and A. J. Ridley.** 1997. Requirement for rho in integrin signaling. Cell Adhes. Commun. **4:**387–398.
5. **Bershadsky, A. D., I. S. Tint, A. A. Neyfakh, Jr., and J. M. Vasiliev.** 1985. Focal contacts of normal and RSV-transformed quail cells. Hypothesis of the transformation-induced deficient maturation of focal contacts. Exp. Cell Res. **158:**433–444.
6. **Birge, R. B., B. S. Knudsen, D. Besser, and H. Hanafusa.** 1996. SH2- and SH3-containing adaptor proteins: redundant or independent mediators of intracellular signal transduction. Gene Cell **1:**595–613.
7. **Bokoch, G. M., B. P. Bohl, and T.-H. Chuang.** 1994. Guanine nucleotide exchange regulates membrane translocation of rac/rho GTP-binding proteins. J. Biol. Chem. **269:**31674–31679.
8. **Burridge, K., and M. Chrzanowska-Wodnicka.** 1996. Focal adhesions, contractility, and signaling. Annu. Rev. Cell Biol. **12:**463–519.
9. **Burridge, K., C. E. Turner, and L. H. Romer.** 1992. Tyrosine phosphorylation of paxillin and $pp125^{FAK}$ accompanies cell adhesion to extracellular matrix: a role in cytoskeletal assembly. J. Cell Biol. **119:**893–903.
10. **Cerione, R. A., and Y. Zheng.** 1996. The dbl family of oncogenes. Curr. Opin. Cell Biol. **8:**216–222.
11. **Chong, L. D., A. Traynor-Kaplan, G. M. Bokoch, and M. A. Schwartz.** 1994. The small GTP-binding protein Rho regulates a phosphatidylinositol 4-phosphate 5-kinase in mammalian cells. Cell **79:**507–513.
12. **Chou, M. M., and J. Blenis.** 1996. The 70 kDa S6 kinase complexes with and is activated by the Rho family G proteins Cdc42 and Rac1. Cell **85:**573–583.
13. **Chrzanowska-Wodnicka, M., and K. Burridge.** 1996. Rho-stimulated contractility drives the formation of stress fibers and focal adhesions. J. Cell Biol. **133:**1403–1415.
14. **Crespo, P., K. E. Schuebel, A. A. Ostrom, J. S. Gutkind, and X. R. Bustelo.** 1997. Phosphotyrosine-dependent activation of rac-1 GDP/GTP exchange by the vav proto-oncogene product. Nature (London) **385:**169–172.
15. **Delannet, M., F. Martin, B. Bossy, D. A. Cheresh, L. F. Reichardt, and J. L. Duband.** 1994. Specific roles of the alpha V beta 1, alpha V beta 3, and alpha V beta 5 integrins in avian neural crest cell adhesion and migration on vitronectin. Development **120:**2687–2702.
16. **Fath, K. R., C.-J. S. Edgell, and K. Burridge.** 1989. The distribution of distinct integrins in focal contacts is determined by the substratum composition. J. Cell Sci. **92:**67–75.
17. **Feller, S. M., B. Knudsen, T. W. Wong, and H. Hanafusa.** 1995. Detection of SH3 binding proteins in total cell lysates with GST-SH3 fusion proteins. Methods Enzymol. **255:**369–378.
18. **Flinn, H. M., and A. J. Ridley.** 1996. Rho stimulates tyrosine phosphorylation of focal adhesion kinase, p130, and paxillin. J. Cell Sci. **109:**1133–1141.
19. **Frisch, S. M., K. Vuori, E. Ruoslahti, and P. Chan-Hui.** 1996. Control of adhesion-dependent cell survival by focal adhesion kinase. J. Cell Biol. **134:**793–799.
20. **Gebbink, M. F. B. G., O. Kranenburg, M. Poland, F. P. G. van Horck, B. Houssa, and W. H. Moolenaar.** 1997. Identification of a novel, putative Rho-specific GDP/GTP exchange factor and a RhoA-binding protein: control of neuronal morphology. J. Cell Biol. **137:**1603–1613.
21. **Gilmore, A. P., and K. Burridge.** 1996. Regulation of vinculin binding to talin and actin by phosphatidyl inositol 4,5-bisphosphate. Nature (London) **381:**531–535.
22. **Glassman, R. H., B. L. Hempstead, L. Stainco-Coico, M. G. Steiner, H. Hanafusa, and R. B. Birge.** 1997. v-Crk, an effector of the NGF signaling pathway, delays apoptotic cell death in neurotrophin-deprived PC12 cells. Cell Death Differ. **4:**82–93.
23. **Gotoh, T., S. Hattori, S. Nakamura, H. Kitayama, M. Noda, Y. Takai, K. Kaibuchi, H. Matsui, O. Hatase, H. Takahashi, T. Kurata, and M. Matsuda.** 1995. Identification of Rap1 as a target for the Crk SH3 domain-binding guanine nucleotide-releasing protein C3G. Mol. Cell. Biol. **15:**6746–6753.
24. **Gulbins, E., K. M. Coggeshell, G. Baier, S. Katzav, P. Burn, and A. Altman.** 1993. Tyrosine kinase stimulated guanine nucleotide exchange activity of vav in T cell activation. Science **260:**822–825.
25. **Hall, A.** 1994. Small GTP-binding proteins and the regulation of the actin cytoskeleton. Annu. Rev. Cell Biol. **10:**31–54.
26. **Hanks, S. K., and T. R. Polte.** 1997. Signaling through focal adhesion kinase. Bioessays **19:**137–145.
27. **Hartwig, J. H., G. M. Bokoch, C. L. Carpenter, P. A. Janmey, L. A. Taylor, A. Toker, and T. P. Stossel.** 1995. Thrombin receptor ligation and activated rac uncap actin filament barbed ends through phosphoinositide synthesis in permeabilized human platelets. Cell **82:**643–653.
28. **Hempstead, B. L., R. B. Birge, J. E. Fajardo, R. Glassman, D. Mahadeo, R. Kraemer, and H. Hanafusa.** 1994. Expression of the v-Crk oncogene product in PC12 cells results in rapid differentiation by both nerve growth factor-dependent and epidermal growth factor-dependent pathways. Mol. Cell Biol. **14:**1964–1971.
29. **Hotchin, N. A., and A. Hall.** 1995. The assembly of integrin adhesion complexes requires both extracellular matrix and intracellular rho/rac GTPases. J. Cell Biol. **131:**1857–1865.
30. **Hungerford, J. E., M. T. Compton, M. L. Matter, B. G. Hoffstom, and C. A. Otey.** 1996. Inhibition of pp125FAK in cultured fibroblasts results in apoptosis. J. Cell Biol. **135:**1383–1390.
31. **Ishizaki, T., M. Maekawa, K. Fujisawa, K. Okawa, A. Iwamatsu, A. Fujita, N. Watanabe, Y. Saito, A. Kakizuka, N. Morii, and S. Narumiya.** 1996. The small GTP-binding protein rho binds to and activates a 160 kDa Ser/Thr protein kinase homologous to myotonic dystrophy kinase. EMBO J. **15:**1885–1893.
32. **Ishizaki, T., M. Naito, K. Fuzisawa, M. Maekawa, N. Watarabe, Y. Saito, and S. Narumiya.** 1997. p160 rock, a rho-associated coiled-coil forming protein kinase, works downstream of rho and induces focal adhesions. FEBS Lett. **404:**118–124.
33. **Jalink, K., and W. H. Moolenaar.** 1992. Thrombin receptor activation causes rapid cell rounding and neurite retraction independent of classic second messengers. J. Cell Biol. **118:**411–419.
34. **Jalink, K., E. J. VanCorven, T. Hengeveld, N. Morii, S. Narumiya, and W. H. Moolenaar.** 1994. Inhibition of lysophosphatidate- and thrombin-induced neurite retraction and neuronal cell rounding by ADP ribosylation of the small GTP-binding protein rho. J. Cell Biol. **126:**801–810.
35. **Janmey, P. A., and T. P. Stossel.** 1987. Modulation of gelsolin function by phosphatidylinositol-4,5-bisphosphate. Nature (London) **325:**362–365.
36. **Kimura, K., M. Ito, M. Amano, K. Chihara, Y. Fukata, M. Nakafuku, B. Yamamori, J. Feng, T. Nakano, K. Okawa, A. Iwamatsu, and K. Kaibuchi.** 1996. Regulation of myosin phosphatase by rho and rho-associated kinase (rho-kinase). Science **273:**245–248.
37. **Knudsen, B. S., S. M. Feller, and H. Hanafusa.** 1994. Four proline-rich sequences of the guanine-nucleotide exchange factor C3G bind with unique specificity to the first src homology 3 domain of Crk. J. Biol. Chem. **269:**32781–32787.
38. **Kozma, R., S. Sarner, S. Ahmed, and L. Lim.** 1997. Rho family GTPases and

neuronal growth cone remodelling: relationship between increased complexity induced by Cdc42Hs, Rac1, and acetylcholine and collapse induced by RhoA and lysophosphatidic acid. Mol. Cell. Biol. **17:**1201–1211.
39. **Kumagai, N., N. Morii, K. Fujisawa, Y. Nemoto, and S. Narumiya.** 1993. ADP-ribosylation of Rho p21 inhibits lysophosphatidic acid-induced protein tyrosine phosphorylation and phosphatidylinositol 3-kinase activation in Swiss 3T3 cells. J. Biol. Chem. **268:**24535–24538.
40. **Lamoureux, P., Z. F. Altun-Gultekin, C. Lin, J. A. Wagner, and S. R. Heideman.** 1997. Rac is required for growth cone function but not neurite assembly. J. Cell Sci. **110:**635–641.
41. **Leberer, E., D. Y. Thomas, and M. Whiteway.** 1997. Pheromone signalling and polarized morphogenesis in yeast. Curr. Opin. Genet. Dev. **7:**59–66.
42. **Leung, T., X.-Q. Chen, E. Manser, and L. Lim.** 1996. The p160 RhoA-binding kinase ROKα is a member of a kinase family and is involved in the reorganization of the cytoskeleton. Mol. Cell. Biol. **16:**5313–5327.
43. **Leung, T., E. Manser, L. Tan, and L. Lim.** 1995. A novel serine/threonine kinase binding the ras-related rhoA GTPase which translocates the kinase to peripheral membranes. J. Biol. Chem. **270:**29051–29054.
44. **Luo, L., T. K. Hensch, L. Ackerman, S. Barbel, L. Y. Jan, and Y. N. Jan.** 1996. Differential effects of the rac GTPase on Purkinje cell axons and dendritic trunks and spines. Nature (London) **379:**837–840.
45. **Luo, L., L. Y. Jan, and Y.-N. Jan.** 1997. Rho family small GTP-binding proteins in growth cone signalling. Curr. Opin. Neurobiol. **7:**81–86.
46. **Luo, L., Y. J. Liao, J. Y. Jan, and Y. N. Jan.** 1994. Distinct morphogenetic functions of similar small GTPases: Drosophilia Drac1 is involved in axonal outgrowth and myoblast fusion. Genes Dev. **8:**1787–1802.
47. **Mackay, D. J. G., C. D. Nobes, and A. Hall.** 1995. The Rho's progress: a potential role during neuritogenesis for the Rho family of GTPases. Trends Neurosci. **18:**496–501.
48. **Madaule, P., T. Furuyashiki, T. Reid, T. Ishizaki, G. Watanabe, N. Morii, and S. Narumiya.** 1995. A novel partner for the GTP-bound forms of rho and rac. FEBS Lett. **377:**243–248.
49. **Manser, E., T. Leung, H. Salihuddin, Z. Zhao, and L. Lim.** 1994. A brain serine/threonine protein kinase activated by Cdc42 and Rac1. Nature (London) **367:**40–46.
50. **Matsui, T., M. Amano, T. Yamamoto, K. Chiara, M. Nakafulu, M. Ito, T. Nakano, K. Okawa, A. Iwamatsu, and K. Kaibuchi.** 1996. Rho-associated kinase, a novel serine/threonine kinase, as a putative target for the small GTP-binding protein rho. EMBO J. **15:**2208–2216.
51. **Mayer, B. J., and H. Hanafusa.** 1990. Mutagenic analysis of the v-*crk* oncogene: requirement for SH2 and SH3 domains and correlation between increased cellular phosphotyrosine and transformation. J. Virol. **64:**3581–3589.
52. **Meier, T., and H. Leying.** 1996. A laboratory guide to biotin-labeling in biomolecule analysis. Birkhauser, Basel, Switzerland.
53. **Miyamoto, S., H. Teramoto, O. A. Coso, J. S. Gutkind, P. D. Burbelo, S. K. Akiyama, and K. M. Yamada.** 1995. Integrin function: molecular hierarchies of cytoskeletal and signaling molecules. J. Cell Biol. **131:**791–805.
54. **Nievers, M., R. B. Birge, H. Greulich, A. J. Verkleif, H. Hanafusa, and P. M. P. van Bergen en Henegouwen.** 1996. v-Crk induced cell transformation: changes in focal adhesion composition and signaling. J. Cell Sci. **110:**389–399.
55. **Nishiki, T., S. Narumiya, N. Morii, M. Yamamoto, M. Fujiwara, Y. Kamata, G. Sakaguchi, and S. Kozaki.** 1990. ADP-ribosylation of the rho/rac proteins induces growth inhibition, neurite outgrowth and acetylcholine esterase in cultured PC12 cells. Biochem. Biophys. Res. Commun. **167:**265–272.
56. **Nobes, C. D., and A. Hall.** 1995. Rho, rac and cdc42 GTPases regulate the assembly of multimolecular focal complexes associated with actin stress fibers, lamellipodia, and filopodia. Cell **81:**53–62.
57. **Nobes, C. D., P. Hawkins, L. Stephens, and A. Hall.** 1995. Activation of the small GTP-binding proteins rho and rac by growth factor receptors. J. Cell Sci. **108:**225–233.
58. **Plopper, G. E., H. P. McNamee, L. E. Dike, K. Bojanowski, and D. E. Ingber.** 1995. Convergence of integrin and growth factor receptor signaling pathways within the focal adhesion complex. Mol. Biol. Cell **6:**1349–1365.
59. **Reid, T., T. Furuyashiki, T. Ishizaki, G. Watanabe, N. Watanabe, K. Fujisawa, N. Morii, P. Madaule, and S. Narumiya.** 1996. Rhotekin, a new putative target for Rho bearing homology to a serine/threonine kinase, PKN, and rhophilin in the rho-binding domain. J. Biol. Chem. **271:**13556–13560.
60. **Ren, X.-D., G. M. Bokoch, A. Traynor-Kaplan, G. H. Jenkins, R. A. Anderson, and M. A. Schwartz.** 1996. Physical association of the small GTPase rho with a 68-kDa phosphatidylinositol 4-phosphate 5-kinase in Swiss 3T3 cells. Mol. Biol. Cell **7:**435–442.
61. **Ridley, A. J., and A. Hall.** 1994. Signal transduction pathways regulating rho-mediated stress fibre formation: requirement for a tyrosine kinase. EMBO J. **13:**2600–2610.
62. **Ridley, A. J., and A. Hall.** 1992. The small GTP binding protein rho regulates the assembly of focal adhesions and stress fibers in response to growth factors. Cell **70:**389–399.
63. **Rossino, P., I. Gavazzi, R. Timpl, M. Aumailley, M. Abbadini, F. Giancotti, L. Silengo, P. C. Marchisio, and G. Tarone.** 1990. Nerve growth factor induces increased expression of a laminin-binding integrin in rat pheochromocytoma PC12 cells. Exp. Cell Res. **189:**100–108.
64. **Schlaepfer, D. D., M. A. Broome, and T. Hunter.** 1997. Fibronectin-stimulated signaling from a focal adhesion kinase–c-Src complex: involvement of the Grb2, p130^{cas}, and Nck adaptor proteins. Mol. Cell. Biol. **17:**1702–1713.
65. **Seckl, M. J., N. Morii, S. Narumiya, and E. Rozengurt.** 1995. Guanosine 5′-3′-O-(thio)triphosphate stimulates tyrosine phosphorylation of p125FAK and paxillin in permeabilized Swiss 3T3 cells. J. Biol. Chem. **270:**6984–6990.
66. **Suidan, H. S., S. R. Stone, B. A. Hemmings, and D. Monard.** 1992. Thrombin causes neurite retraction in neural cells through activation of cell surface receptors. Neuron **8:**363–375.
67. **Tahagi, J., T. Kamata, J. Meredith, W. Puzon-McLaughlin, and Y. Takada.** 1997. Changing ligand specificities of $\alpha_V\beta_1$ and $\alpha_V\beta_3$ integrins by swapping a short diverse sequence of the β subunit. J. Biol. Chem. **272:**19796–19800.
68. **Tanaka, S., T. Morishita, Y. Hashimoto, S. Hattori, S. Nakamura, M. Shibuya, K. Matuoka, T. Takenawa, T. Kurata, K. Nagashima, and M. Matsuda.** 1994. C3G, a guanine nucleotide-releasing protein expressed ubiquitously, binds to the Src homology 3 domains of CRK and GRB2/ASH proteins. Proc. Natl. Acad. Sci. USA **91:**3443–3447.
69. **Tanaka, S., T. Ouchi, and H. Hanafusa.** 1997. Downstream of Crk adaptor signaling pathway: activation of Jun kinase by v-Crk through the guanine nucleotide exchange protein C3G. Proc. Natl. Acad. Sci. USA **94:**2356–2361.
70. **Teng, K. K., H. Lander, J. E. Fajardo, H. Hanafusa, B. L. Hempstead, and R. B. Birge.** 1995. v-crk modulation of growth factor-induced PC12 cell differentiation involves the src homology 2 domain of v-crk and sustained activation of the Ras/mitogen-activated protein kinase pathway. J. Biol. Chem. **270:**20677–20685.
71. **Tigyi, G., D. J. Fischer, A. Sebok, C. Yang, D. L. Dyer, and R. Miledi.** 1996. Lysophosphatidic acid-induced neurite retraction in PC12 cells: control by phosphoinositide-Ca^{2+} signaling and rho. J. Neurochem. **66:**537–548.
72. **Tigyi, G., and R. Miledi.** 1992. Lysophosphatidates bound to serum albumin activate membrane currents in Xenopus oocytes and neurite retraction in PC12 pheochromocytoma cells. J. Biol. Chem. **267:**21360–21367.
73. **Tomaselli, K. J., D. E. Hall, L. A. Flier, K. R. Gehlsen, D. C. Turner, S. Carbonetto, and L. F. Reichardt.** 1990. A neuronal cell line (PC12) express two β_1-class integrins—$\alpha_1\beta_1$ and $\alpha_3\beta_1$—that recognize different neurite outgrowth-promoting domains in laminin. Neuron **5:**651–662.
74. **Vincent, S., and J. Settleman.** 1997. The PRK2 kinase is a potential effector target of both Rho and Rac GTPases and regulates actin cytoskeletal organization. Mol. Cell. Biol. **17:**2247–2256.
75. **Watanabe, G., Y. Saito, P. Madaule, T. Ishizaki, K. Fujisawa, N. Morii, H. Mukai, Y. Ono, and A. Kakizuka.** 1996. Protein kinase N (PKN) and PKN-related protein rhophilin as targets of small GTPase rho. Science **271:**645–648.
76. **Watanabe, N., P. Madaule, T. Reid, T. Ishizaki, G. Watanabe, A. Kakizuka, Y. Saito, K. Nakao, B. M. Jockusch, and S. Narumiya.** 1997. p140mDia, a mammalian homolog of Drosophila diaphanous, is a target protein for rho small GTPase and is a ligand for profilin. EMBO J. **16:**3044–3056.
77. **Zachary, I., J. Sinnett-Smith, C. E. Turner, and E. Rozengurt.** 1993. Bombesin, vasopressin, and endothelin rapidly stimulate tyrosine phopshorylation of the focal adhesion-associated protein paxillin in Swiss 3T3 cells. J. Biol. Chem. **268:**22060–22065.
78. **Zhang, Z., G. Tarone, and D. C. Turner.** 1993. Expression of integrin α1 β1 is regulated by nerve growth factor and dexamethasone in PC12 cells. Functional consequences for adhesion and neurite outhgrowth. J. Biol. Chem. **268:**5557–5565.
79. **Zheng, Y., D. Zangrilli, R. A. Cerione, and A. Eva.** 1996. The pleckstrin homology domain mediates transformation by oncogenic dbl through specific intracellular targeting. J. Biol. Chem. **271:**19017–19020.